Journal of Organometallic Chemistry 694 (2009) 703–716

Contents lists available at ScienceDirect

Journal of Organometallic Chemistry

journal homepage: www.elsevier.com/locate/jorganchem

# Group 4 metal complexes bearing new tridentate (NNO) ligands: Benzyl migration and formation of unusual C–C coupled products

Renan Cariou, Vernon C. Gibson *, Atanas K. Tomov, Andrew J.P. White

*Department of Chemistry, Imperial College London, Exhibition Road, London SW7 2AZ, UK*

ARTICLE INFO

*Article history:*
Received 24 September 2008
Received in revised form 21 November 2008
Accepted 28 November 2008
Available online 7 December 2008

*Keywords:*
Group 4 metal complexes
Intramolecular benzyl migration
Carbon–carbon coupling
Ethylene polymerization

ABSTRACT

Group 4 metal complexes bearing new phenoxy(benzimidazolyl)-imine, -amine and -amide ligands have been synthesized. A series of metal chloride derivatives has been prepared via treatment of $MCl_4(THF)_2$ (M = Ti, Zr, Hf) with the *in situ* generated sodium salt of the (benzimidazolyl)imine phenol **1**. Reaction of the pro-ligand **2** with $TiCl_4(THF)_2$ afforded the corresponding complex **8** in which the amine proton remains bound to the nitrogen donor. Benzyl complexes of zirconium and hafnium were synthesized via treatment of pro-ligands **1** and **2** with $M(CH_2Ph)_4$ precursors. The complexes $[NNO]M(CH_2Ph)_3$ (**6** M = Zr, **7** **M** = Hf) were found to undergo benzyl migration from the metal centre to the imine carbon of the ligand backbone giving complexes **11** and **12**; the migration follows first order kinetics. The reaction of **1** with $Ti(NMe_2)_4$ led to the formation of an unusual C–C coupled product in which a new piperazine ring has formed. Complexes **11** and **12** undergo related transformations, leading to analogous C–C coupled products which were characterized by X-ray crystallography. Deuterium labelling experiments were carried out to determine the mechanistic pathway of the reactions. Chloride and benzyl complexes **3–12** were screened as pre-catalysts for olefin polymerization.



## 1. Introduction

Over the past twenty years, academic and industrial research programmes have successfully targetted new catalysts for controlled olefin polymerization. Numerous highly active single-site homogeneous catalysts based on metals across the transition series have been reported [1,2]. While many different donor groups have been explored, there are certain types, steric affects aside, that seem to be specially suited to the stabilization of high activity catalysts. Among these are imine and phenoxy donors and especially a combination of these two donors (I, Chart 1) [3–29]. In recent studies, we have found that benzimidazole donors can also afford exceptionally active catalysts (II, Chart 1) [30,31]. We were, therefore, attracted by the possibility of combining phenoxy, imine and benzimidazolyl donors within a single tridentate ligand system with a view to seeing if the beneficial affects of these donors might be retained within an extended ligand frame. Here, we report, the synthesis and characterization of a family of Group 4 metal complexes bearing the new phenoxy(benzimidazolyl)-imine and phenoxy(benzimidazolyl)amide ligands, their unusual benzyl migration reactivity to give C–C coupled products, along with their ethylene polymerization behavior.

## 2. Results and discussion

### 2.1. Pro-ligand synthesis

Pro-ligand **1** was synthesized in moderate yield using a modified literature procedure [34], via condensation of 3,5-di-*tert*-butylsalicyladehyde with 2-aminomethyl-1-methylbenzimidazole dihydrochloride in the presence of $K_2CO_3$ (Scheme 1).

The $^1$H NMR spectrum of **1** shows characteristic signals for the $^t$Bu substituents, at 1.28 and 1.41 ppm, and resonances for the imine hydrogen and the aromatic protons of the phenol unit at 8.54 and 13.10 ppm, respectively. The methylene bridge resonates as a doublet at 5.09 ppm due to a small $^3J_{HH}$ coupling of 1.2 Hz to the amine proton.

Reaction of **1** with 2.0 equivalents of $^t$BuLi, followed by aqueous work-up, afforded the pro-ligand **2**, in which the imine has been reduced to a secondary amine (Scheme 1). Consistently, the $^1$H NMR spectrum of **2** revealed an ABX coupling pattern centered at 3.98 ppm attributable to the presence of diastereotopic methylene bridge protons. The amine proton was found to resonate at 2.86 ppm as a doublet of doublet resonance again due to coupling to the two diastereotopic protons of the $CH_2$ group.

* Corresponding author. Tel.: +44 02075945830; fax: +44 02075945810.
*E-mail addresses:* v.gibson@imperial.ac.uk, v.gibson@ic.ac.uk (V.C. Gibson).

0022-328X/$ - see front matter © 2008 Elsevier B.V. All rights reserved.
doi:10.1016/j.jorganchem.2008.11.064

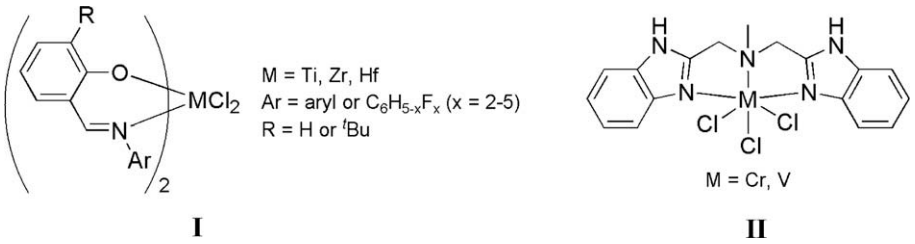


**Chart 1.** Bis(phenoxyimine) and bis(benzimidazolyl)amine pre-catalysts.

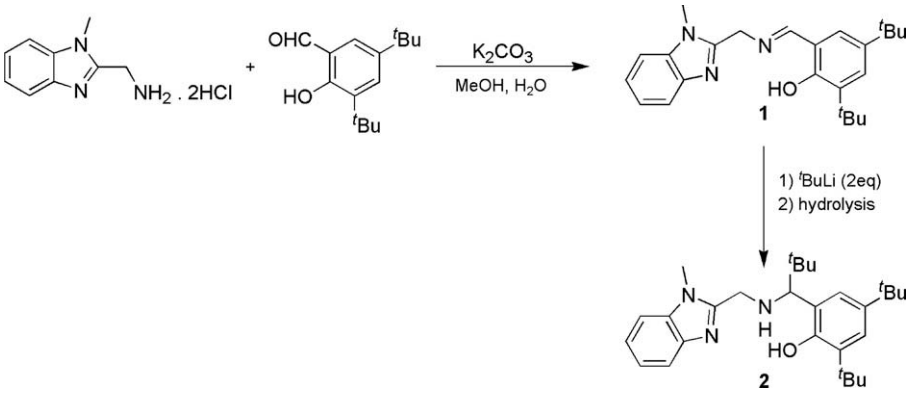


**Scheme 1.** Synthesis of pro-ligands **1** and **2**.

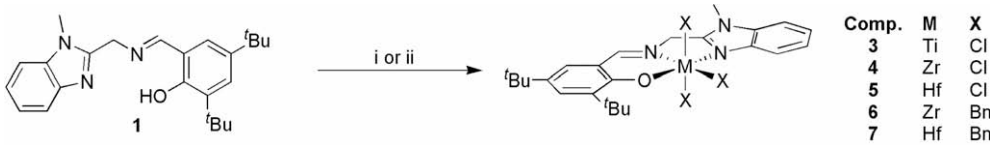


**Scheme 2.** Synthesis of complexes ((i) NaH in THF, then $MCl_4(THF)_2$; (ii) $M(CH_2Ph)_4$ in toluene at RT).

### 2.2. Synthesis and structure of metal chloride derivatives

**1** was converted to its sodium salt using NaH and immediately reacted with $MCl_4(THF)_2$ (M = Ti, Zr, Hf) to afford the desired chloride complexes **3, 4** and **5** (Scheme 2).

$^1$H NMR spectra of these complexes showed a characteristic peak for the imine proton in the region 8.5–8.7 ppm. Complexes **3** and **5** display singlet resonances at *ca.* 5.60 ppm assignable to the equivalent protons of the methylene bridge indicating that the ligand is coordinated in a meridional fashion. For **4**, an additional small coupling of 1.4 Hz is observed between the methylene bridge and the imine proton.

Single crystals of **3** suitable for X-ray analysis were grown from a saturated acetonitrile solution.

The solid state structure was found to contain four crystallographically independent complexes, (**A–D**) with essentially identical geometries except for the positions of the methyl carbons of the *t*-butyl groups; complex **3-A** is shown in Fig. 1, complexes **3-B, 3-C** and **3-D** are shown in Figs. S2–S8. The geometry at the metal centre is distorted octahedral with the tridentate ligand coordinated in a meridional fashion, and with the Ti–Cl bond *trans* to N(8) noticeably shorter than those *trans* to chlorine (Table 1). The six-membered *N,O* and the five-membered *O,O′* chelate rings are both flat and coplanar, a planarity that extends to include the fused ring systems; with the exception of Cl(1), Cl(2) and the two *t*-butyl groups, the whole of the complex is approximately planar with mean deviations of *ca.* 0.05, 0.06, 0.06 and 0.06 Å for **3-A, 3-B, 3-C** and **3-D**, respectively [35].

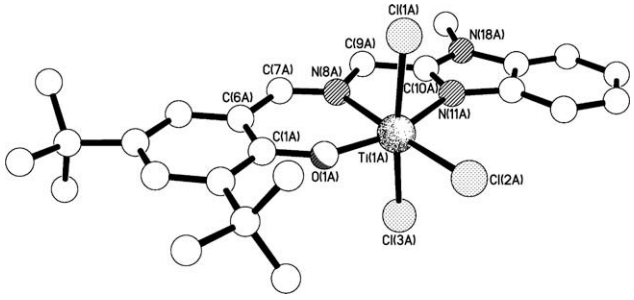


**Fig. 1.** The molecular structure of **3-A**, one of the four. crystallographically independent complexes present in the crystals of **3**.

The reaction of **2** with $TiCl_4(THF)_2$ in THF at room temperature led to the formation of the trichloride complex **8** (Scheme 3). The ligand appears to be monoanionic and tridentate, in which the amine proton remains bonded to the central nitrogen donor. This proton resonates as a broad doublet resonance at 4.90 ppm with coupling (by COSY NMR) to the diastereotopic methylene protons as well as with the methine proton on the adjacent carbon atoms. Slow cooling of a saturated toluene solution led to the formation of single crystals suitable for X-ray analysis.

**Table 1**
Comparative selected bond lengths (Å) and angles (°) for the four crystallographically independent complexes present in the crystals of **3**.

| | 3-A | 3-B | 3-C | 3-D |
|---|---|---|---|---|
| Ti(1)–Cl(1) | 2.3403(11) | 2.3516(11) | 2.3357(11) | 2.3357(11) |
| Ti(1)–Cl(2) | 2.2929(11) | 2.2973(11) | 2.2880(11) | 2.2870(11) |
| Ti(1)–Cl(3) | 2.3450(11) | 2.3266(11) | 2.3390(11) | 2.3331(11) |
| Ti(1)–O(1) | 1.790(2) | 1.797(2) | 1.791(2) | 1.797(2) |
| Ti(1)–N(8) | 2.180(3) | 2.175(3) | 2.169(3) | 2.193(3) |
| Ti(1)–N(11) | 2.145(3) | 2.157(3) | 2.168(3) | 2.144(3) |
| C(7)–N(8) | 1.296(4) | 1.282(4) | 1.276(5) | 1.280(4) |
| N(8)–C(9) | 1.470(4) | 1.469(4) | 1.479(4) | 1.475(5) |
| Cl(1)–Ti(1)–Cl(2) | 91.46(4) | 91.09(4) | 91.19(4) | 91.52(4) |
| Cl(1)–Ti(1)–Cl(3) | 168.65(4) | 169.70(4) | 168.56(4) | 169.24(4) |
| Cl(1)–Ti(1)–O(1) | 94.94(8) | 94.07(8) | 94.76(8) | 94.05(8) |
| Cl(1)–Ti(1)–N(8) | 87.91(8) | 88.68(8) | 86.96(8) | 88.52(8) |
| Cl(1)–Ti(1)–N(11) | 84.25(8) | 84.44(8) | 84.98(8) | 84.36(8) |
| Cl(2)–Ti(1)–Cl(3) | 92.06(4) | 92.21(4) | 92.76(4) | 91.79(4) |
| Cl(2)–Ti(1)–O(1) | 101.05(9) | 101.52(8) | 101.28(8) | 100.53(8) |
| Cl(2)–Ti(1)–N(8) | 176.76(9) | 176.45(8) | 176.13(9) | 177.81(9) |
| Cl(2)–Ti(1)–N(11) | 102.26(9) | 101.77(8) | 101.80(9) | 103.18(9) |
| Cl(3)–Ti(1)–O(1) | 94.97(8) | 94.82(8) | 94.99(8) | 95.40(8) |
| Cl(3)–Ti(1)–N(8) | 87.98(8) | 87.43(8) | 88.43(8) | 87.79(8) |
| Cl(3)–Ti(1)–N(11) | 84.46(8) | 85.34(8) | 83.70(8) | 84.91(8) |
| O(1)–Ti(1)–N(8) | 82.18(11) | 82.03(11) | 82.28(11) | 81.65(11) |
| O(1)–Ti(1)–N(11) | 156.69(12) | 156.69(11) | 156.93(11) | 156.27(11) |
| N(8)–Ti(1)–N(11) | 74.51(11) | 74.68(11) | 74.66(11) | 74.65(11) |

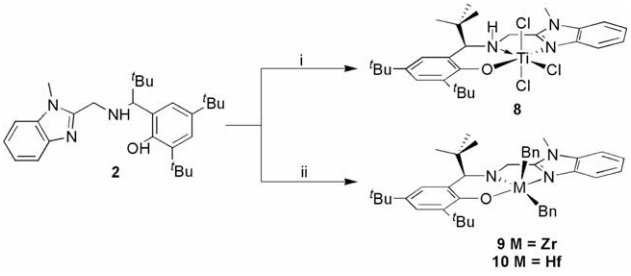


**Scheme 3.** Legend: (i) $TiCl_4(THF)_2$ in THF; (ii) $M(CH_2Ph)_4$ in toluene at RT.

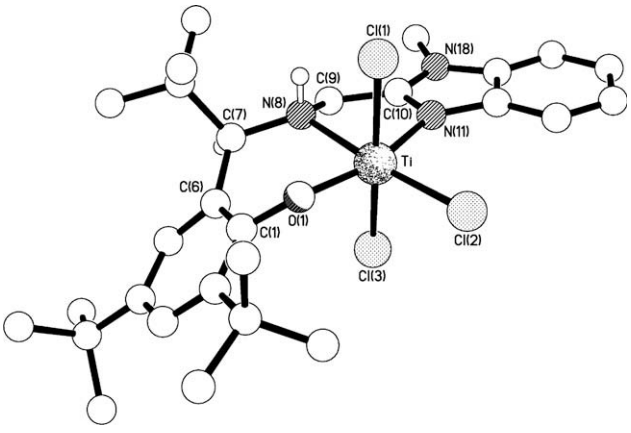


**Fig. 2.** The molecular structure of **8**.

The change from an $sp^2$ geometry for the N(8) nitrogen in **3** to an $sp^3$ geometry for the same nitrogen in **8** leads to a very marked change in the conformation of the ligand (Fig. 2). Although the ligand is coordinated in a meridional fashion to the octahedral metal centre, the six-membered *N,O* chelate ring has a distorted folded conformation [O(1) and C(1) lying *ca.* 0.77 and 0.48 Å, respectively out of the {Ti,C(6),C(7),N(8)} plane which is coplanar to within *ca.* 0.07 Å] that results in the C(1)/C(6) aromatic $C_6$ ring being inclined by *ca.* 42° to the equatorial {Ti,Cl(2),O(1),N(8),N(11)} plane. The five-membered *N,N′* chelate ring is also distorted away from planarity, having an envelope conformation with N(8) lying *ca.* 0.42 Å out of the {Ti,C(9),C(10),N(11)} plane which is coplanar to within *ca.* 0.02 Å. The bonds to the metal atom (Table 2) show the same pattern as seen in the structure of **3**, though here the difference between the two Ti–N bonds is much clearer as a result in the change in the hybridisation of N(8).

**Table 2**
Selected bond lengths (Å) and angles (°) for **8**.

| | | | |
|---|---|---|---|
| Ti–Cl(1) | 2.3487(13) | Ti–Cl(2) | 2.2730(11) |
| Ti–Cl(3) | 2.3384(13) | Ti–O(1) | 1.787(3) |
| Ti–N(8) | 2.249(3) | Ti–N(11) | 2.139(3) |
| C(7)–N(8) | 1.513(4) | N(8)–C(9) | 1.478(4) |
| Cl(1)–Ti–Cl(2) | 92.66(5) | Cl(1)–Ti–Cl(3) | 171.97(5) |
| Cl(1)–Ti–O(1) | 94.52(9) | Cl(1)–Ti–N(8) | 87.61(10) |
| Cl(1)–Ti–N(11) | 88.68(9) | Cl(2)–Ti–Cl(3) | 92.54(5) |
| Cl(2)–Ti–O(1) | 104.68(9) | Cl(2)–Ti–N(8) | 172.76(10) |
| Cl(2)–Ti–N(11) | 97.66(9) | Cl(3)–Ti–O(1) | 90.08(9) |
| Cl(3)–Ti–N(8) | 86.47(10) | Cl(3)–Ti–N(11) | 84.55(9) |
| O(1)–Ti–N(8) | 82.50(12) | O(1)–Ti–N(11) | 157.24(11) |
| N(8)–Ti–N(11) | 75.11(12) | | |

### 2.3. Synthesis and structure of metal benzyl derivatives

NMR scale reactions of compounds **1** and **2** with (separately) $Zr(CH_2Ph)_4$ and $Hf(CH_2Ph)_4$ proceeded cleanly in $C_6D_6$ and indicated quantitative conversion into the corresponding tribenzyl complexes **6** and **7** (from **1**) and the dibenzyl complexes **9** and **10** (from **2**) as well as affording toluene as a by-product (Schemes 2 and 3). Reactions on a preparative scale were carried out in toluene at room temperature to afford **6** and **7** as orange, and **9** and **10** as white, microcrystalline powders. The $^1H$ NMR spectrum of **6** revealed a pair of AB doublets centered at 2.77 and 2.94 ppm integrating for four protons and assigned to diastereotopic benzyl protons ($^2J_{HH}$ = 9.2 Hz). A singlet at 3.25 ppm was assigned to equivalent protons of a third benzyl group. The aromatic region of the spectrum revealed signals attributable to the *ortho*-protons of the benzyl phenyl unit to relatively high-field (5.90–6.40 ppm), suggesting $\eta^2$-coordination at the metal centre. This is supported by a relatively low $^2J_{HH}$ value of 9.2 Hz for the diastereotopic protons of the $CH_2Ph$ groups and a $^1J_{CH}$ value of 126 Hz. [36–40] The methylene bridge of the ligand appears as a singlet at 2.67 ppm indicating that the ligand is coordinated in a meridional fashion, in accord with the NMR observations of the chloride complexes. An analogous $^1H$ NMR spectrum was observed for the corresponding hafnium derivative, **7**.

The dibenzyl complexes **9** and **10** have essentially similar $^1H$ NMR spectra and show no fluxionality at room temperature. In **10**, the benzylic protons resonate as two sets of AB doublets centered at 1.55, 2.18 and 2.44, 2.86 ppm ($^2J_{HH}$ = 11.1 Hz, $^2J_{HH}$ = 11.3 Hz). The corresponding benzyl carbons appear as triplets at 65.7 and 67.3 ppm, in the $^1H$-coupled $^{13}C$ NMR spectrum, with $^1J_{CH}$ values of 122 and 127 Hz, respectively, values that suggest that the benzyl units are bonded in $\eta^2$-fashion.

Single crystals of the hafnium derivative **10** were grown from a toluene solution at −20 °C. The solid state structure showed the presence of two crystallographically independent complexes, (**A** and **B**) with broadly similar geometries (the major exception being the C(51) phenyl ring); complex **10-A** is shown in Fig. 3, complex **10-B** in Fig. S13, and an overlay of the two complexes is shown in Fig. S15. The geometry at the five-coordinate hafnium centre is intermediate between square-based pyramidal (sbp) and trigonal bipyramidal (tbp) as indicated by $\tau$ parameter [41] values of

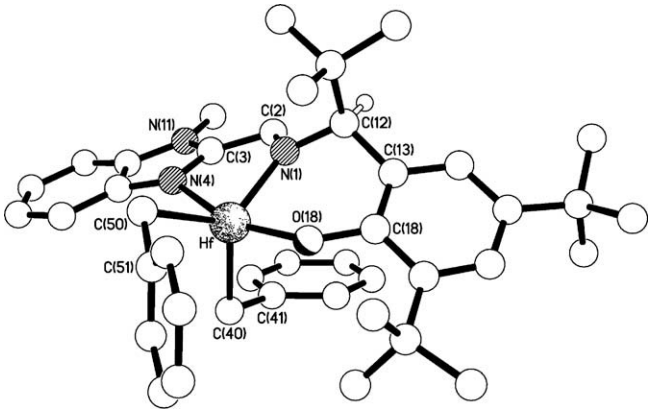


**Fig. 3.** The molecular structure of **10-A**, one of the two crystallographically independent complexes present in the crystals of **10**.

**Table 3**
The square-based pyramidal/trigonal bipyramidal parameter $\tau$ for the solid state structures of complexes **10-A, 10-B, 14, 15** and **16**.[a]

| | A | $\alpha$ (°) | $\beta$ (°) | $\tau$ [$\tau = (\beta - \alpha)/60°$] |
|---|---|---|---|---|
| 10-A | C(40) | 126.76(13) | 158.03(9) | 0.52 |
| 10-B | C(40) | 124.62(12) | 158.48(9) | 0.56 |
| 14 | N(31) | 129.28(6) | 161.09(8) | 0.53 |
| 15 | C(30) | 125.92(6) | 157.41(6) | 0.52 |
| 16 | C(30) | 126.83(7) | 158.55(5) | 0.53 |

[a] Donor **A** defined as being the atom not involved in either of the two largest angles at the metal centre; angles $\beta$ and $\alpha$ are the largest and second largest angles at the metal centre, respectively.

0.52 and 0.56 for **10-A** and **10-B**, respectively (Table 3). The two equatorial Hf–C bond lengths are identical within error (Table 4), but it is interesting to note that the Hf–C–C(Ph) angle at C(50) in complex **10-B** is *ca.* 7° smaller than the other three, suggesting a degree of $\eta^2$-coordination for this benzyl ligand [the Hf···C(51) separation is 2.879(3) Å in complex **10-B** *cf.* 2.994(3) Å in **10-A**]. It is unclear, however, why this effect should be present in only one of the two independent complexes as there are no other significant conformational differences, and the closest *intra* and *inter*molecular approaches to the centroid of the C(51) phenyl ring are shorter for complex **10-A** than for complex **10-B** [42].

The geometry at the amido nitrogen is significantly flattened, N(1) lying only *ca.* 0.08 Å [0.11 Å] out of the plane of its substituents (the value in square parentheses refers to complex **10-B**), compared to *ca.* 0.36 Å for the equivalent nitrogen [N(8)] in the structure of **8**. Associated with this is a shortening of the N–C(H)(*t*-Bu) bond from 1.513(4) Å for C(7)–N(8) in **8**, to 1.467(4) Å [1.482(4) Å] for N(1)–C(12) in **10**, suggesting a degree of $sp^2$ hybridisation. The most noticeable effect, however, is seen in the Hf–N bond lengths with that to N(1) *ca.* 0.25 Å shorter than that to the $sp^2$ nitrogen N(4), though part of this will be due to a lengthening of the Hf–N(4) bond caused by N(4) occupying a *pseudo*-axial position (if the metal coordination geometry is viewed as tbp, N(4) and O(18) would be in the axial sites) *trans* to a phenoxide donor.

This flattening of the geometry at the amino nitrogen results in an overall flattening of the tridentate ligand *cf.* the conformation seen in **8**. Here in **10** the C(13)/C(18) aromatic $C_6$ ring is inclined to the {Hf,N(1),N(4),O(18)} plane by *ca.* 30° [35°] *cf. ca.* 42° in **8**. The six-membered *N,O* chelate ring has a boat conformation with C(12) and O(18) lying *ca.* 0.48 [0.44] and 0.28 Å [0.36 Å] out of the {Hf,N(1),C(13),C(18)} plane which is coplanar to within *ca.* 0.02 Å [0.03 Å]. The five-membered *N,N′* chelate ring has a envelope geometry with the metal lying *ca.* 0.62 Å [0.48 Å] out of the {N(1),C(2),C(3),N(4)} plane which is coplanar to better than 0.01 Å [0.01 Å].

### 2.4. Intramolecular benzyl migration reactions

Zirconium benzyl complexes are known to undergo benzyl migration processes [43]. Scott and coworkers reported that titanium and zirconium benzyl complexes bearing bridged phenoxyimine ligands can undergo migrations of one of the benzyls to the imino carbon of the ligand backbone [19,44–46]. Other systems based on pyrrolylimines and α-diimine ligands show similar reactivities [47–50]. We have found that **6** and **7** also undergo benzyl transfer reactions in solution leading to the corresponding dibenzyl complexes **11** and **12** (Scheme 4).

Typically, three different benzyl signals are observed in $^1$H NMR of complexes **11** and **12**: two sets of AB doublets for the benzyl groups bound the metal centre and an ABC multiplet for the protons of the benzyl group attached to the ligand backbone. The methylene bridge protons are diastereotopic and appear as an AB system. As observed in **9** and **10**, the aromatic protons of one of the benzyl ligands appear upfield (6.10–6.50 ppm) indicative of $\eta^2$-coordination. The $^1$H NMR spectrum of the starting tribenzyl complex **6** and the product **11** following benzyl migration are shown in Fig. 4.

The transformation of **6** to **11** occurred over several hours and thus could be conveniently followed by $^1$H NMR spectroscopy. The reaction followed first order kinetics with a $k_{obs}$ value of $2.3 \times 10^{-4}$ s$^{-1}$ at 313 K ($t_{1/2}$ = 50 min) (Fig. 5). The conversion of **7** into **12** proceeds a little slower, with a $k_{obs}$ value of $4.3 \times 10^{-5}$ s$^{-1}$ at 313 K ($t_{1/2}$ = 271 min). Eyring plots revealed negative $\Delta S^{\#}$ values (−79 and −139 J K$^{-1}$ mol$^{-1}$, respectively for the conversion of **6** into **11** and **7** into **12**; Fig. 6) indicative of non-dissociative intramolecular processes [46].

The corresponding titanium tribenzyl complex could not be accessed since the reaction of **1** with Ti($CH_2Ph$)$_4$ in an NMR scale reac-

**Table 4**
Comparative selected bond lengths (Å) and angles (°) for the two crystallographically independent complexes present in the crystals of **10**.

| | 10-A | 10-B | | 10-A | 10-B |
|---|---|---|---|---|---|
| Hf–N(1) | 2.056(3) | 2.063(2) | Hf–N(4) | 2.319(3) | 2.301(3) |
| Hf–O(18) | 1.952(2) | 1.950(2) | Hf–C(40) | 2.270(3) | 2.276(3) |
| Hf–C(50) | 2.267(3) | 2.276(3) | N(1)–C(2) | 1.454(4) | 1.444(4) |
| N(1)–C(12) | 1.467(4) | 1.482(4) | | | |
| N(1)–Hf–N(4) | 73.75(10) | 73.68(10) | N(1)–Hf–O(18) | 84.84(10) | 85.43(9) |
| N(1)–Hf–C(40) | 113.03(12) | 111.68(11) | N(1)–Hf–C(50) | 126.76(13) | 124.62(12) |
| N(4)–Hf–O(18) | 158.03(9) | 158.48(9) | N(4)–Hf–C(40) | 84.17(11) | 83.87(11) |
| N(4)–Hf–C(50) | 92.30(11) | 92.82(11) | O(18)–Hf–C(40) | 100.18(11) | 99.53(11) |
| O(18)–Hf–C(50) | 104.66(12) | 103.49(11) | C(40)–Hf–C(50) | 116.28(14) | 120.04(13) |
| Hf–C(40)–C(41) | 105.7(2) | 104.9(2) | Hf–C(50)–C(51) | 104.1(2) | 97.8(2) |

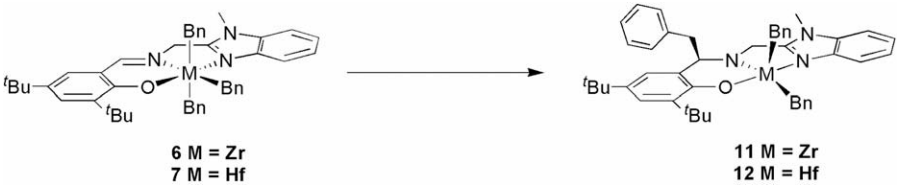


**Scheme 4.**

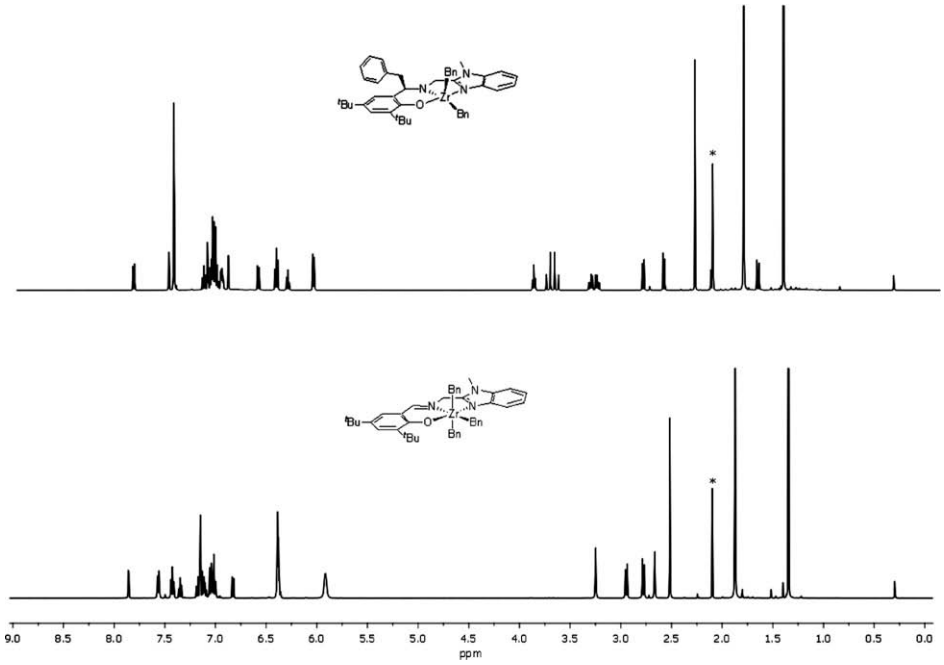


**Fig. 4.** $^1$H NMR ($C_6D_6$) spectra of **6** and **11**.

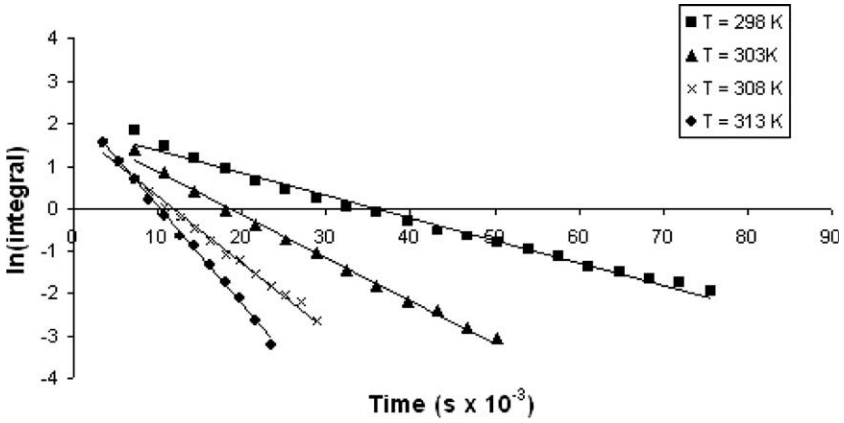


**Fig. 5.** First order plots for the conversion of **6** into **11** at various temperatures.

tion afforded a mixture of unidentified products, while the reaction of **3** with $PhCH_2MgCl$ in THF afforded exclusively the migration product **13** (Scheme 5). Compound **13** possesses the same NMR features as its zirconium and hafnium congeners **11** and **12**. A key difference, however, is that **13** decomposes rapidly in solution at room temperature to give an unusual C–C coupled product. The nature of this species will be probed in the following section.

### 2.5. Formation of unusual C–C coupled products

#### 2.5.1. From reaction with $Ti(NMe_2)_4$

Compound **1** reacted with $Ti(NMe_2)_4$ in a NMR scale reaction (in $C_6D_6$) to liberate free dimethylamine and give a new complex (**14**; Scheme 6). The compound has low solubility in $C_6D_6$ and precipitated out of the solution after a few hours. Single crystals suitable

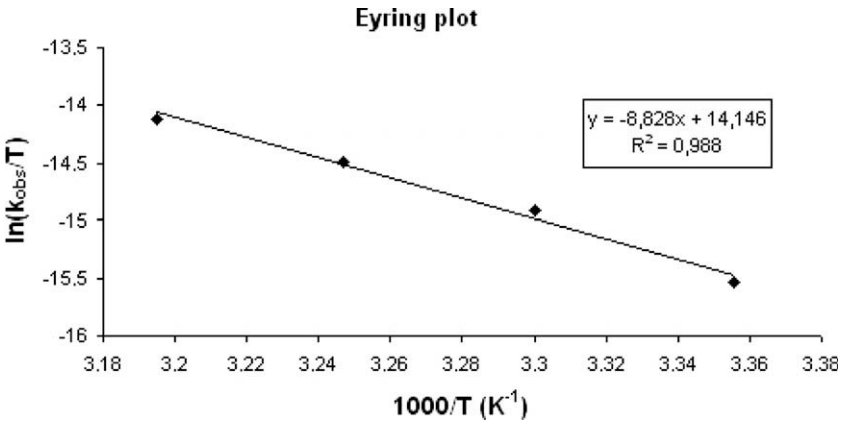


**Fig. 6.** Eyring plot of the transformation of **6** into **11**.

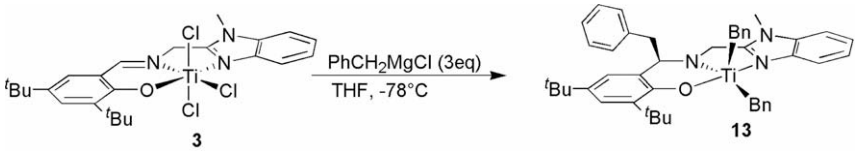


**Scheme 5.**

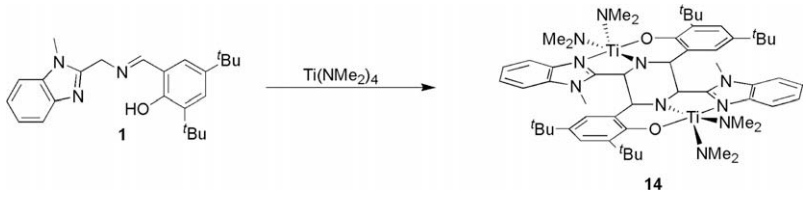


**Scheme 6.** NMR scale reaction of **1** with $Ti(NMe_2)_4$ in $C_6D_6$.

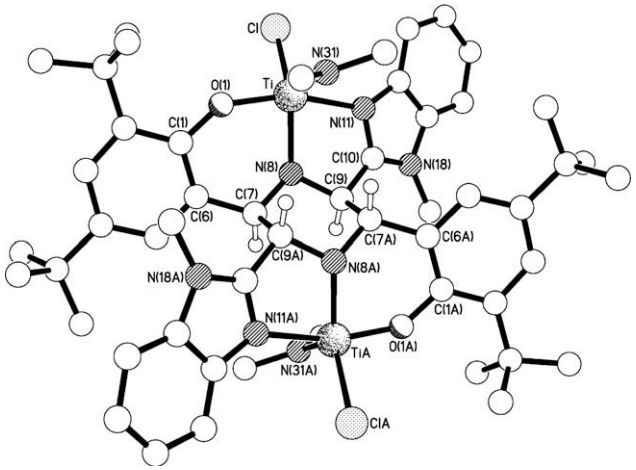


**Fig. 7.** The molecular structure of the $C_i$-symmetric complex **14**.

for X-ray analysis could be grown from a $CD_2Cl_2$ solution; the molecular structure is shown in Fig. 7.

The X-ray analysis revealed an unexpected $C_i$-symmetric dinuclear species, formed by the back-to-back cross-coupling of the imine bonds of two adjacent complexes (Fig. 4). To our knowledge only two other examples of such coupling have been reported [51,52], this being the first example with a Group 4 metal. The resulting central piperazine $C_4N_2$ ring has a chair conformation with the four carbon atoms perfectly planar (a consequence of the centre of symmetry at the middle of the ring) and the nitrogens lying *ca.* 0.71 Å out of, and on opposite sides of this plane. The pyramidalisation of the N(8) centre is intermediate between those seen for the equivalent nitrogens in the structures of **8** and **10**, the nitrogen here in **14** sitting *ca.* 0.28 Å out of the plane of its substituents, *cf. ca.* 0.36, 0.08 and 0.11 Å in **8, 10-A** and **10-B**, respectively. That this nitrogen has retained significant $sp^2$ character is also shown by the two N(8)–C bonds being the same (Table 5) and similar to those seen in **10**.

The $\tau$ parameter value of 0.53 shows that the geometry at the metal centre is intermediate between sbp and tbp (Table 3), with O(1) and N(11) occupying the *pseudo*-axial sites. The six-membered N,*O* chelate ring has a distorted folded geometry, Ti and N(8) lying *ca.* 0.55 and 0.69 Å, respectively out of the {O(1),C(1),C(6),C(7)} plane which is coplanar to within *ca.* 0.02 Å. The five-membered *N,N′* chelate ring has an envelope conformation with C(9) lying *ca.* 0.42 Å out of the {Ti,N(8),C(10),N(11)} plane which is coplanar to within *ca.* 0.04 Å. The tridentate ligand has a flatter conformation here in **14** than seen in either **8** or **10**, the C(1)/C(6) aromatic $C_6$ ring here being inclined by *ca.* 19° to the {Ti,O(1),N(8),N(11)} plane *cf. ca.* 42, 30 and 35° in **8, 10-A** and **10-B**, respectively.

**Table 5**
Selected bond lengths (Å) and angles (°) for **14**.

| | | | |
|---|---|---|---|
| Ti–Cl | 2.3029(8) | Ti–O(1) | 1.8219(17) |
| Ti–N(8) | 1.9909(19) | Ti–N(11) | 2.179(2) |
| Ti–N(31) | 1.898(2) | C(7)–N(8) | 1.468(3) |
| N(8)–C(9) | 1.460(3) | C(7)–C(9A) | 1.577(3) |
| Cl–Ti–O(1) | 99.06(6) | Cl–Ti–N(8) | 129.28(6) |
| Cl–Ti–N(11) | 86.54(5) | Cl–Ti–N(31) | 113.98(7) |
| O(1)–Ti–N(8) | 86.28(7) | O(1)–Ti–N(11) | 161.09(8) |
| O(1)–Ti–N(31) | 99.11(9) | N(8)–Ti–N(11) | 76.35(7) |
| N(8)–Ti–N(31) | 114.80(8) | N(11)–Ti–N(31) | 94.97(9) |

Plausible mechanistic pathways for the formation of **14** are shown in Scheme 7. The free dimethylamine formed during the complexation of **1** could deprotonate the ligand backbone either at the methylene bridge or at the imine carbon. If deprotonation occurs at the imine, the imine carbon will be negatively charged and a 1,3-hydrogen shift of a methylene proton may then occur (Scheme 7, route A). The alternative pathway proceeds via deprotonation of the methylene bridge (Scheme 7 route B).

Deuterium labelling experiments were conducted to identify the site of deprotonation. Pro-ligand **1*d*$_2$**, in which the methylene bridge protons are substituted by deuterium atoms, was synthesized and reacted with $Ti(NMe_2)_4$ on an NMR scale in $C_6D_6$. Two products can be envisaged from this reaction: **14*d*$_4$** in which the ring is entirely deuterated and **14*d*$_2$** in which the ring is "half-deuterated", with the protons and deuterons lying opposite to each other (Scheme 8).

If the mechanism occurs via route A (deprotonation at the imine followed by a 1,3-hydrogen shift), **14*d*$_4$** will be formed and no signals attributable to the piperazine ring will be observable in the $^1$H NMR spectrum. By contrast, should the reaction proceed via route B (deprotonation at the methylene bridge), **14*d*$_2$** will be formed and the $^1$H NMR spectrum will then show a singlet resonance integrating for two protons. The $^1$H NMR spectrum of the product of the reaction showed one singlet at 4.51 ppm, corresponding to **14*d*$_2$**, thus indicating that the reaction occurs via route B.

### 2.5.2. From benzyl complexes

Complexes **11** and **12**, arising from benzyl migration, appear to undergo a further transformation in solution over a period of several weeks. Indeed, while attempting to grow crystals of **11** and **12** for X-ray analysis, we discovered that the crystals formed were in fact the new complexes **15** and **16**. A single crystal X-ray diffraction study **15** revealed a structure analogous to that of the titanium species **14**, but with the chloro and dimethylamino ligands in the latter replaced by a pair of benzyl groups (Fig. 8). The complex is again centrosymmetric, and the piperazine ring has a chair conformation (the four carbon atoms are perfectly coplanar and the nitrogens lie *ca.* 0.72 Å out of this plane on opposite sides). The N(8) nitrogen atom is markedly less pyramidalised than seen in **14**, here sitting only *ca.* 0.16 Å out of the plane of its substituents *cf. ca.* 0.28 Å in **14**.

The most interesting aspect of this structure is the difference between the coordination of the C(30) and C(40) benzyl ligands. Whilst the C(40) ligand binds in an $\eta^1$ fashion with a Zr–C(40)–C(41) angle of 106.71(12)°, the equivalent angle at C(30) is *ca.* 11° smaller [Zr–C(30)–C(31) 95.76(13)°]. Associated with this is a *ca.* 0.2 Å reduction in the Zr···C(31) separation [2.832(2) Å] *cf.* that to C(41) [3.0568(19) Å]; the Zr–C(30) and Zr–C(40) bond lengths are the same (Table 6). This clearly points to a significant $\eta^2$ interaction for the C(30) benzyl ligand. Interestingly, the "inner" face of the C(41) phenyl ring is involved in a pair of intramolecular C–H···$\pi$ contacts, the protons on C(7A) and C(9A) being *ca.* 2.94

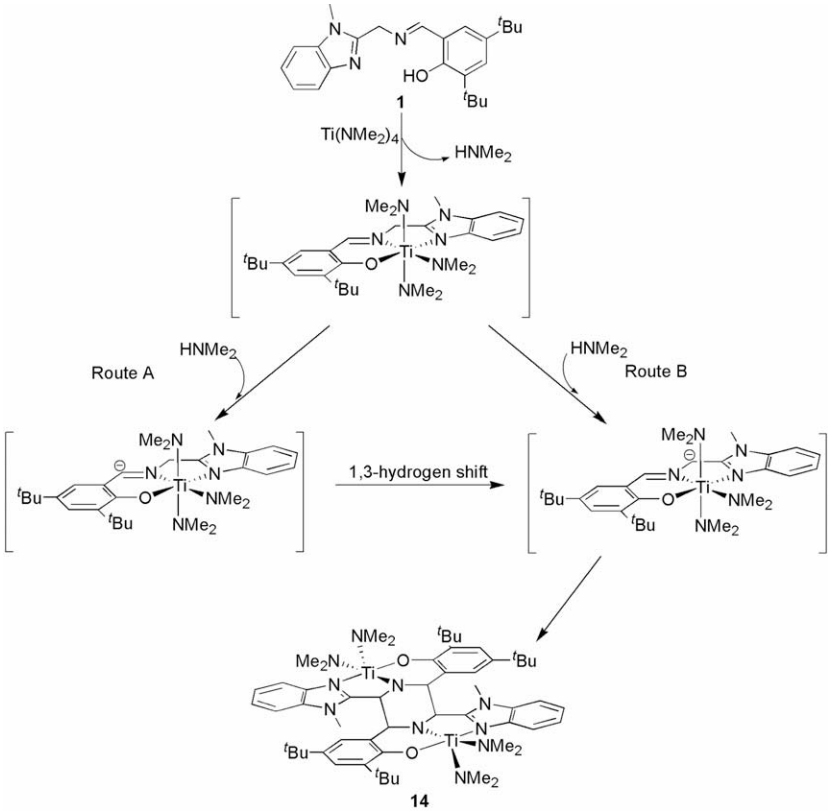


**Scheme 7.** Plausible mechanism for the formation of **14**.

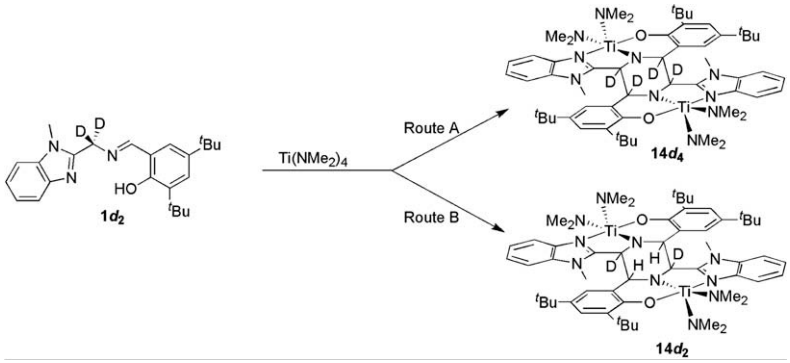


**Scheme 8.** Possible products of the reaction between $\mathbf{1d_2}$ and $Ti(NMe_2)_4$.

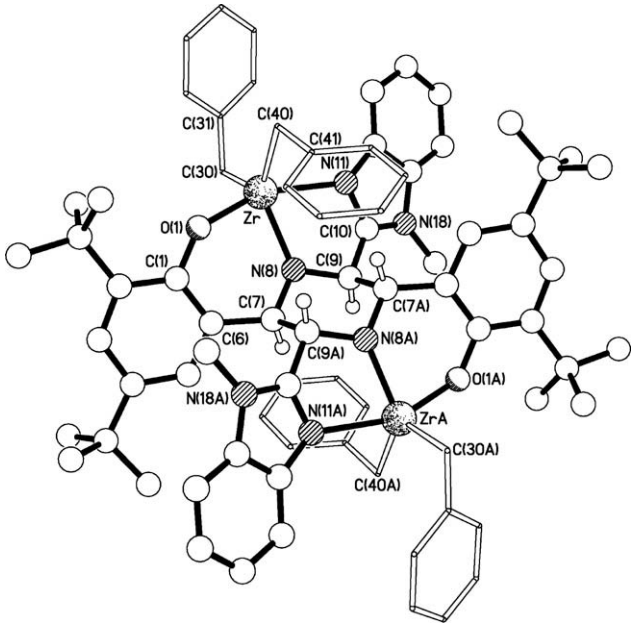


**Fig. 8.** The molecular structure of the $C_i$-symmetric complex **15**.

**Table 6**
Selected bond lengths (Å) and angles (°) for **15**.

| | | | |
|---|---|---|---|
| Zr–O(1) | 1.9650(13) | Zr–N(8) | 2.1058(15) |
| Zr–N(11) | 2.2952(15) | Zr–C(30) | 2.278(2) |
| Zr–C(40) | 2.2861(18) | C(7)–N(8) | 1.469(2) |
| N(8)–C(9) | 1.469(2) | C(7)–C(9A) | 1.581(2) |
| O(1)–Zr–N(8) | 84.32(5) | O(1)–Zr–N(11) | 157.41(6) |
| O(1)–Zr–C(30) | 99.45(7) | O(1)–Zr–C(40) | 97.51(6) |
| N(8)–Zr–N(11) | 74.25(6) | N(8)–Zr–C(30) | 111.26(7) |
| N(8)–Zr–C(40) | 125.92(6) | N(11)–Zr–C(30) | 94.99(7) |
| N(11)–Zr–C(40) | 89.54(6) | C(30)–Zr–C(40) | 121.48(7) |
| Zr–C(30)–C(31) | 95.76(13) | Zr–C(40)–C(41) | 106.71(12) |

and 3.19 Å from the ring centroid. The closest approach to the C(31) ring centroid is from a methyl proton on the N(18)–Me group in an adjacent complex to the "outer" face of the C(31) phenyl ring with an H···π separation of *ca.* 3.22 Å.

Comparing the titanium (**14**) to the zirconium complex (**15**), the bonds between the metal and O(1), N(8) and N(11) are all lengthened by *ca.* 0.12 Å in the zirconium derivative, and there is an associated *ca.* 4° contraction of the O(1)–Zr–N(11) angle. As was the case for **10-A, 10-B** and **14**, the geometry at the metal centre here in **15** is again intermediate between sbp and tbp as shown by a $\tau$ value of 0.52 (Table 3).

The six-membered *N,O* chelate ring has a boat geometry, O(1) and C(7) lying *ca.* 0.21 and 0.32 Å, respectively out of the {Zr,C(1),C(6),N(8)} plane which is coplanar to within *ca.* 0.02 Å. The five-membered *N,N′* chelate ring has an envelope conformation with C(10) lying *ca.* 0.31 Å out of the {Zr,N(8),C(9),N(11)} plane which is coplanar to within *ca.* 0.05 Å. The tridentate ligand has a flatter conformation than seen in **14**, with here the C(1)/C(6) aromatic $C_6$ ring here being inclined by *ca.* 15° to the {Zr,O(1), N(8),N(11)} plane *cf. ca.* 19° in **14**.

The structure of **16** is isomorphous with that of its Zr analogue (see Supplementary material). If the complexes **15** and **16** arise from **11** and **12**, two molecules of toluene must be formed during the process. Therefore, we considered a radical mechanism for the formation of these C–C coupled products, the initiation step involving homolytic cleavage of the C–$CH_2$Ph bond, leading to the formation of a benzyl radical and a radical species **A** in which the radical character is retained by the ligand. The benzyl radical can attack the ligand (at the methylene bridge) on another complex molecule to form a new radical species **B**. Coupling of the radical **A** and **B** occurs leading to the intermediate **C**. Further cleavage of the remaining benzyl carbon bond would lead to the second coupling step (Scheme 9).

In order to probe this mechanistic hypothesis, the reaction of $\mathbf{1d_2}$ with $Zr(CH_2Ph)_4$was followed. The order of the reaction was determined to be 3/2, consistent with Rice–Herzfeld radical propagation kinetics [53,54], with rate constants of $2.75 \times 10^{-5}$ $mol^{-0.5}\,L^{1.5}\,min^{-1}$ and $1.48 \times 10^{-5}\,mol^{-0.5}\,L^{1.5}\,min^{-1}$ for **11** and $\mathbf{11d_2}$, respectively. Furthermore, the ratio of the rate constants $k_H/k_D$ is 1.8, a value corresponding to a secondary kinetic isotope effect. This suggests that, if a C–H (C–D) bond is broken during the reaction, it is not the rate-determining step. Therefore the homolytic cleavage of the C–$CH_2$Ph bond can be reasonably considered the rate-determining step. In addition, formation of toluene is observed during the decomposition of both complexes. According to the mechanism proposed in Scheme 9, $d_1$-toluene should be formed during the decomposition of $\mathbf{11d_2}$; a $^2$H NMR spectrum confirmed the formation of $d_1$-toluene (see Supplementary material). Furthermore, a small quantity of bibenzyl is observed, a consequence of benzyl radical coupling, and consistent with the proposed radical pathway. An example of the dissociation of a carbon-benzyl (C–$CH_2$Ph) bond has been reported for a coenzyme $B_{12}$ model complex; in this system a benzyl group migrates reversibly from the cobalt centre to the imine carbon of the ligand. It was found that the bond dissociation energy of the carbon-benzyl (C–$CH_2$Ph) bond was about one third lower than that of a normal carbon-benzyl bond [55–59].

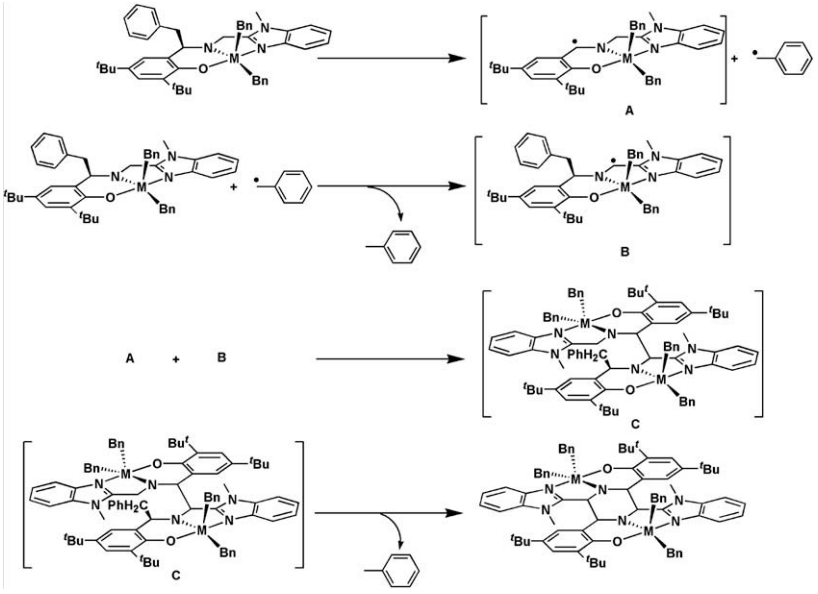

**Scheme 9.** Postulated mechanism for the formation of **15** and **16**.

**Table 7**
Ethylene polymerization results.

| Entry | Pre-catalyst[a] | Co-catalyst | $T$ (°C) | Yield (g) | Activity[b] | $M_n$[c] (g mol$^{-1}$) | $M_w$[c] (g mol$^{-1}$) | PDI |
|---|---|---|---|---|---|---|---|---|
| 1 | **3** | MAO (500 eq) | 25 | Trace | – | – | – | – |
| 2 | **4** | MAO (500 eq) | 25 | – | – | – | – | – |
| 3 | **5** | MAO (500 eq) | 25 | | – | – | – | – |
| 4 | **3** | Al($^i$Bu)$_3$/DMAO[d] | 25 | 0.55 | 150 | 10 300 | 493 200 | 47.9 |
| 5 | **3** | Al($^i$Bu)$_3$/DMAO[d] | 50 | 0.50 | 133 | 19 400 | 450 200 | 23.2 |
| 6 | **8** | MAO (500 eq) | 25 | – | – | – | – | – |
| 7 | **8** | Al($^i$Bu)$_3$/DMAO[d] | 25 | Trace | – | – | – | – |

*Conditions*: Schlenk, toluene (200 ml); 1.5 bar ethylene; 30 min.
[a] Pre-catalyst loading: 5 μmol.
[b] Activity in g mmol$^{-1}$ h$^{-1}$ bar$^{-1}$.
[c] Determined by GPC.
[d] Al($^i$Bu)$_3$/Ti = 100, DMAO/Ti = 200.

### 2.6. Ethylene polymerization tests

Complexes **3–12** were investigated as catalyst precursors for ethylene polymerization. Among the chloride pre-catalysts, **3** showed only trace activity upon activation with MAO. However, when Al($i$Bu)$_3$/DMAO (TMA free) was used as cocatalyst, an activity of 150 g mmol$^{-1}$ h$^{-1}$ bar$^{-1}$ was obtained. The resulting polyethylene has a molecular weight of about Mw of ~500 000 g mol$^{-1}$ with a broad molecular weight distribution (Table 7). In contrast, **4** and **5** were inactive under these conditions. The benzyl complexes of zirconium and hafnium, **6**, and **9–12**, were also inactive upon activation with MAO or Al($i$Bu)$_3$/[Ph$_3$ C][B(C$_6$F$_5$)$_4$].

## 3. Conclusion

In summary, we have synthesized and characterized a series of new Group 4 metal complexes bearing tridentate (NNO) ligands. It was found that benzyl derivatives undergo ready migration of a benzyl ligand from the metal centre to the imine carbon of the ligand backbone. Unusual dinuclear C–C coupled complexes were identified as products of decomposition and an analogous product was obtained from a titanium-amido precursor. The mechanism of the coupling processes have been elucidated using deuterium labelling experiments and found to proceeds via a radical pathway for the benzyl complexes and via deprotonation of the ligand backbone by *in situ* formed free dimethylamine in the case of the amido-titanium system. The reactivity of the ligand backbone may account for the poor performance of these complexes in ethylene polymerization.

## 4. Experimental

All manipulations of air and moisture sensitive compounds were carried out under an atmosphere of $N_2$ using standard Schlenk techniques or by using a conventional nitrogen-filled glove box. Diethyl ether was distilled under nitrogen, over sodium benzophenone ketyl. THF was distilled under nitrogen, over potassium. Dichloromethane was dried and distilled over calcium hydride under an atmosphere of nitrogen. Toluene and pentane, were dried by passing through a column filled with commercially available Q-5 reactant (Cu(II)O on alumina 13% w/w) and activated alumina (pellets, 3 mm) and stored over a potassium mirror. Glycine-2-$d_2$ ethyl ester hydrochloride [60], 2-aminomethyl-1-methylbenzimidazole dihydrochloride [61], $TiCl_4(THF)_2$ [62], $ZrCl_4(THF)_2$ [62], $HfCl_4(THF)_2$ [62], $Zr(CH_2Ph)_4$ [63] and $Hf(CH_2Ph)_4$ [63] were prepared according to published procedures. 3,5-di-*tert*-Butyl-salicylaldehyde, and

$Ti(NMe_2)_4$ were purchased from Aldrich and used without further purification. Ethylene (CP grade) was purified by passing it through an Oxy-trap and gas drier (Alltech Associates). MAO was purchased from Chemtura. NMR spectra were recorded on Bruker, DRX-400, Avance-400, Avance-500 spectrometers. IR spectra were recorded on a Perkin–Elmer spectrum 1760X FT-IR spectrometer. Elemental analyses were performed by the microanalytical services at London Metropolitan University. Mass spectra were recorded on a VG Autospec or a VG Platform II spectrometer.

### 4.1. Synthesis of pro-ligands

#### 4.1.1. NNO (**1**)

2-aminomethyl-1-methylbenzimidazole dihydrochloride (2.00 g, 8.55 mmol) was dissolved in 5 mL of distilled water and neutralized with potassium carbonate (1.18 g, 8.55 mmol). A stirred solution of 3,5-di-*tert*-butyl-salicylaldehyde (2.00 g, 8.55 mmol) in 15 ml of methanol was added dropwise and the mixture stirred for 12 h at room temperature. A yellow solid precipitated out of the solution. The solid was filtered, dried and crystallized from hot acetonitrile to afford a yellow crystalline product. The product was dried at 60 °C under vacuum overnight. Yield = 2.05 g (64%). Anal. Calc. for $C_{24}H_{31}N_3O$ (377.53): C, 76.35; H, 8.28; N, 11.13. Found: C, 76.51; H, 8.30; N, 10.97%. $^1$H NMR (500 MHz, $CDCl_3$, 298 K): $\delta$ 13.10 (s, 1H, O*H*), 8.54 (t, 1H, N=C*H*, $^3J_{HH}$ = 1.2 Hz), 7.76 (d, 1H, Ar*H*), 7.39 (d, 1H, Ar*H*, $^4J_{HH}$ = 2.5 Hz), 7.37 (m, 1H, Ar*H*), 7.31 (dt, 1H, Ar*H*), 7.28 (m, 1H, Ar*H*), 7.09 (d, 1H, Ar*H*, $^4J_{HH}$ = 2.5 Hz), 5.09 (s, 2H, C$H_2$, $^3J_{HH}$ = 1.2 Hz), 3.91 (s, 3H, N-C$H_3$), 1.41 (s, 9H, C(C$H_3$)$_3$), 1.28 (s, 9H, C(C$H_3$)$_3$). $^{13}$C{$^1$H} NMR (126 MHz, $CDCl_3$, 298 K): $\delta$ 169.1 (N=*C*H), 157.7 (*C*q), 150.7 (*C*q), 142.3 (*C*q), 140.5 (*C*q), 136.7 (*C*q), 136.2 (*C*q), 127.7 (Ar*C*H), 126.5 (Ar*C*H), 122.9 (Ar*C*H), 122.3 (Ar*C*H), 119.9 (Ar*C*H), 117.8 (*C*q), 109.4 (Ar*C*H), 55.5 (*C*H$_2$), 35.00 (*C*(CH$_3$)$_3$), 34.1 (*C*(CH$_3$)$_3$), 31.4 (C(*C*H$_3$)), 30.4 (N-*C*H$_3$), 29.4 (C(*C*H$_3$)). MS (positive ES; *m*/*z*): 378 [M−H]$^+$. IR (KBr (s), cm$^{-1}$): 2995 (w), 2955 (s), 2906 (m), 2866 (m), 1625 (s), 1595 (m), 1507 (w), 1473 (s), 1441 (s), 1405 (m), 1393 (w), 1361 (m), 1323 (m), 1287 (w), 1272 (m), 1252 (s), 1243 (m), 1222 (w), 1206 (w), 1175 (m), 1151 (w), 1132 (w), 1059 (w), 1046 (w), 1006 (w), 944 (w), 881 (w), 860 (w), 828 (m), 805 (w), 768 (w), 756 (w), 739 (s), 646 (w), 414 (w).

#### 4.1.2. $^{tBu}$NNO (**2**)

To a solution of **1** (0.788 g, 2.09 mmol) in $Et_2O$ (10 mL) was added *t*-butyllithium (2.8 mL, 4.18 mmol) at −78 °C. The red solution was allowed to warm up slowly to room temperature and stirred for 1 h. The reaction was quenched with a saturated aqueous $NH_4Cl$ solution. The organic phase was separated, washed with $NH_4Cl$, brine; dried over $Na_2SO_4$ and evaporated to dryness. Recrystallisation of the white residue in acetonitrile afforded white needles. Yield = 0.65 g (72%). Anal. Calc. for $C_{28}H_{41}N_3O$ (435.65): C, 77.20; H, 9.49; N, 9.65. Found: C, 77.27; H, 9.41; N, 9.78%. $^1$H NMR (500 MHz, $CDCl_3$, 298 K): $\delta$ 11.61 (s, 1H, O*H*), 7.76 (m, 1H, Ar*H*), 7.30 (m, 3H, Ar*H*), 7.22 (d, 1H, Ar*H*, $^4J_{HH}$ = 2.4 Hz), 6.72 (d, 1H, Ar*H*, $^4J_{HH}$ = 2.4 Hz), 3.98 (m, 2H, C$H_2$, $^2J_{HaHb}$ = 14.1 Hz, $^3J_{HaNH}$ = 5.3 Hz, $^3J_{HbNH}$ = 9.0 Hz), 3.62 (s, 3H, N-C$H_3$), 3.46 (s, 1H, C*H*-$^t$Bu), 2.86 (dd, 1H, N*H*, $^3J_{HaNH}$ = 5.3 Hz, $^3J_{HbNH}$ = 9.0 Hz)), 1.44 (s, 9H, C(C$H_3$)$_3$), 1.29 (s, 9H, C(C$H_3$)$_3$), 0.98 (s, 9H, C(C$H_3$)$_3$). $^{13}$C{$^1$H} NMR (126 MHz, $CDCl_3$, 298 K): $\delta$ 154.3 (*C*q), 152.1 (*C*q), 142.4 (*C*q), 139.1 (*C*q), 135.7 (*C*q), 135.7 (*C*q), 126.7 (Ar*C*H), 122.7 (Ar*C*H), 122.5 (Ar*C*H), 122.2 (Ar*C*), 119.8 (Ar*C*), 119.5 (Ar*C*H), 109.4 (Ar*C*H), 75.0 (*C*H-$^t$Bu), 43.9 (*C*H$_2$), 36.3 (*C*(CH$_3$)$_3$), 34.9 (*C*(CH$_3$)$_3$), 34.0 (*C*(CH$_3$)$_3$), 31.6 (C(*C*H$_3$)$_3$), 29.8 (N-*C*H$_3$), 29.6 (C(*C*H$_3$)$_3$), 27.3 (C(*C*H$_3$)$_3$). MS (positive ES; *m*/*z*): 436 [M−H]$^+$. IR (KBr (s), cm$^{-1}$): 3273 (m), 3060 (w), 2954 (s), 2906 (m), 2866 (m), 1964 (w), 1880 (w), 1616 (w), 1602 (w), 1511 (w), 1478 (s), 1439 (w), 1401 (m), 1359 (m), 1336 (w), 1326(w), 1298 (w), 1287 (w), 1249 (s), 1236 (m), 1203 (m), 1163 (m), 1150 (w), 1130 (w), 1070 (m), 1024 (s), 1009 (w), 996 (m), 921 (w), 888 (w), 866 (w), 824 (m), 767 (w), 740 (s), 727 (w), 696 (m), 650 (w), 575 (w), 507 (w), 436 (w).

### 4.2. Synthesis of complexes

#### 4.2.1. [NNO]$TiCl_3$ (**3**)

To a suspension of NaH (0.035 g, 1.48 mmol) in THF (10 mL) at −78 °C was added a solution of **1** (0.557 g, 1.48 mmol) in THF (10 mL). The reaction was allowed to warm up to room temperature and stirred for 1 h30. The resulting yellow solution was added slowly onto a solution of $TiCl_4(THF)_2$ (0.493 g, 1.48 mmol) in THF (5 mL) at −78 °C. The reaction became red and was left 2 h at room temperature. The solution was filtered, and volatiles were evaporated to afford a red powder. Yield = 0.55 g (70%). Anal. Calc. for $C_{24}H_{30}Cl_3N_3OTi$ (530.74): C, 54.30; H, 5.70; N, 7.92. Found: C, 54.19; H, 5.53; N, 7.81%. $^1$H NMR (500 MHz, THF-$d_8$, 298 K): $\delta$ 8.63 (dd, 1H, Ar*H*), 8.59 (broad s, 1H, N=C*H*), 7.70 (d, 1H, Ar*H*), 7.57 (m, 1H, Ar*H*), 7.49 (d, 1H, Ar*H*), 7.42 (m, 2H, Ar*H* benz), 5.53 (s, 2H, N-C$H_2$), 3.89 (s, 3H, N-CH$_3$), 1.59 (s, 9H, C(CH$_3$)$_3$), 1.36 (s, 9H, C(CH$_3$)$_3$). $^{13}$C{$^1$H} NMR (126 MHz, THF-$d_8$, 298 K): $\delta$ 166.7 (N=*C*H), 159.8 (*C*q), 153.7 (*C*q), 146.2 (*C*q), 138.6 (*C*q), 137.0 (*C*q), 135.8 (*C*q), 131.4 (*C*H), 129.9 (*C*H), 127.2 (*C*q), 124.9 (*C*H), 124.7 (*C*H), 120.5 (*C*H), 110.6 (*C*H), 56.5 (N-*C*H$_2$), 35.9 (*C*(CH$_3$)$_3$), 35.2 (*C*(CH$_3$)$_3$), 31.5 (C(*C*H$_3$)$_3$), 30.9 (N-*C*H$_3$), 30.2 (C(*C*H$_3$)$_3$). IR (KBr (s), cm$^{-1}$): 2956 (s), 2904 (m), 2864 (m), 2357 (w), 1617 (s), 1566 (m), 1505 (m), 1480 (w), 1457 (s), 1416 (m), 1391 (m), 1362 (m), 1316 (m), 1267 (m), 1247 (s), 1210 (w), 1184 (w), 1060 (m), 1008 (w), 934 (w), 919 (w), 905 (w), 870 (s), 760 (s), 618 (w), 603 (w), 578 (m), 497 (s), 410 (m).

#### 4.2.2. [NNO]$ZrCl_3$ (**4**)

An analogous procedure was employed to that described for **3**, using NaH (0.024 g, 1 mmol), **1** (0.376 g, 1.00 mmol) and $ZrCl_4(THF)_2$ (0.375 g, 1.00 mmol). Yield = 0.42g (73%). Anal. Calc. for $C_{24}H_{30}Cl_3N_3OZr$ (574.09): C, 50.21; H, 5.27; N, 7.32. Found: C, 50.08; H, 4.99; N, 7.26%. $^1$H NMR (400 MHz, THF-$d_8$, 298 K): $\delta$ 8.68 (t, 1H, N=C*H*, $^4J_{HH}$ = 1.4 Hz), 8.35 (m, 1H, Ar*H* benz), 7.71 (d, 1H, Ar*H*, $^4J_{HH}$ = 2.5 Hz), 7.64 (m, 1H, Ar*H* benz), 7.46 (m, 2H, Ar*H* benz), 7.42 (d, 1H, Ar*H*, $^4J_{HH}$ = 2.5 Hz), 5.55 (d, 2H, N-C$H_2$, $^4J_{HH}$ = 1.4 Hz), 3.94 (s, 3H, N-C$H_3$), 1.55 (s, 9H, C(C$H_3$)$_3$), 1.35 (s, 9H, C(C$H_3$)$_3$). $^{13}$C{$^1$H} NMR (101 MHz, THF-$d_8$, 298 K): $\delta$ 171.4 (N=*C*H), 157.5 (*C*q), 155.2 (*C*q), 143.9 (*C*q), 138.8 (*C*q), 137.9 (*C*q), 135.8 (*C*q), 132.2 (*C*H), 130.5 (*C*H), 125.3 (*C*H), 125.2 (*C*H), 124.3 (*C*H), 119.7 (*C*H), 111.1 (*C*H), 55.9 (N-*C*H$_2$), 35.9 (*C*(CH$_3$)$_3$), 34.9 (*C*(CH$_3$)$_3$), 31.5 (C(*C*H$_3$)$_3$), 30.9 (N-*C*H$_3$), 30.1 (C(*C*H$_3$)$_3$). IR (KBr (s), cm$^{-1}$): 2958 (s), 2910 (m), 2872 (m), 1611 (s), 1566 (s), 1550 (m), 1506 (s) 1480 (w), 1461 (s), 1416 (s), 1395 (m), 1362 (w), 1321 (w), 1290 (m), 1276 (s), 1252 (s), 1212 (w), 1184 (m), 1136 (w), 1058 (m), 1012 (w), 940 (w), 920 (w), 900 (w), 864 (s), 816 (w), 758 (s), 699 (w), 619 (w), 602 (w), 562 (m), 497 (w), 475 (w), 433 (w), 410 (w).

#### 4.2.3. [NNO]$HfCl_3$ (**5**)

An analogous procedure was employed to that described for **3**, using NaH (0.013 g, 0.53 mmol), **1** (0.201 g, 0.53 mmol) and $HfCl_4(THF)_2$ (0.247 g, 0.53 mmol). Yield = 0.29g (82%). Anal. Calc. for $C_{24}H_{30}Cl_3HfN_3O$ (661.36): C, 43.59; H, 4.57; N, 6.35. Found: C, 43.78; H, 4.60; N, 6.31%. $^1$H NMR (400 MHz, THF-$d_8$, 298 K): $\delta$ 8.68 (broad s, 1H, N=C*H*), 8.37 (m, 1H, Ar*H*), 7.73 (d, 1H, Ar*H*, $^4J_{HH}$ = 2.5 Hz), 7.64 (m, 1H, Ar*H*), 7.46 (m, 2H, Ar*H* benz), 7.41 (d, 1H, Ar*H*, $^4J_{HH}$ = 2.7 Hz), 5.60 (s, 2H, N-C$H_2$), 3.93 (s, 3H, N-C$H_3$), 1.54 (s, 9H, C(C$H_3$)$_3$), 1.34 (s, 9H, C(C$H_3$)$_3$). $^{13}$C{$^1$H} NMR (101 MHz, THF-$d_8$, 298 K): $\delta$ 172.1 (N=CH), 158.2 (*C*q), 156.3 (*C*q), 143.4 (*C*q), 139.6 (*C*q), 138.0 (*C*q), 136.0 (*C*q), 132.6 (*C*H),

130.5 (*C*H), 125.5 (*C*H), 125.3 (*C*H), 124.5 (*C*q), 119.8 (*C*H), 111.3 (*C*H), 55.8 (N-$CH_2$), 35.9 ($C(CH_3)_3$), 35.0 ($C(CH_3)_3$), 31. 7 ($C(CH_3)_3$), 31.1 (N-$CH_3$), 30.2 ($C(CH_3)_3$). IR (KBr (s), $cm^{-1}$): 2956 (s), 2909 (m), 2869 (m), 1612 (s), 1565 (s), 1553 (m), 1506 (m), 1482 (w), 1460 (s), 1419 (s), 1395 (m), 1362 (w), 1321 (m), 1292 (m), 1279 (s), 1254 (m), 1209 (w), 1201 (w), 1183 (m), 1136 (w), 1059 (m), 1010 (w), 939 (w), 919 (w), 902 (w), 864 (s), 773 (m), 756 (s), 700 (w), 643 (w), 616 (w), 605 (w), 557 (m), 492 (w), 475 (w), 433 (w), 410 (w).

#### 4.2.4. [NNO]Zr($CH_2Ph$)$_3$ (**6**)

In a glove box, a solution of the pro-ligand **1** (0.200 g, 0.53 mmol) in toluene (5 mL) was added to a solution of $Zr(CH_2Ph)_4$ (0.241 g, 0.53 mmol) in toluene (5 ml). The resulting solution was stirred at RT for 30 min and volatiles were removed under reduced pressure. The solid residue was washed with cold pentante to afford **6** as an orange powder. Yield = 0.25 g (65%). Anal. Calc. for $C_{45}H_{51}N_3OZr$ (741.14): C, 72.93; H, 6.94; N, 5.67. Found: C, 72.87; H, 6.89; N 5.58%. $^1$H NMR (500 MHz, $C_6D_6$, 283 K): $\delta$ 7.86 (d, 1H, $^3J_{HH}$ = 2.5 Hz, ArH), 7.56 (d, 2H, $^3J_{HH}$ = 7.3 Hz, ArH), 7.42 (t, 2H, $^3J_{HH}$ = 7.7 Hz, ArH), 7.35 (t, 1H, $^3J_{HH}$ = 8.2 Hz, Ar*H*), 7.00–7.20 (m, 5H, 4 Ar*H* + N=C*H*), 6.83 (d, 1H, $^3J_{HH}$ = 8.2 Hz, Ar*H*), 6.38 (m, 6H, *meta* + *para*-$CH_2Ph$), 5.91 (broad s, 4H, *ortho*-$CH_2Ph$), 3.25 (s, 2H, Zr-C$H_2$Ph), 2.94 (d, 2H, $^2J_{HH}$ = 9.2 Hz, Zr-CH(*H*)Ph), 2.77 (d, 2H, $^2J_{HH}$ = 9.2 Hz, Zr-C*H*(H)Ph), 2.67 (s, 2H, NC$H_2$), 2.51 (s, 3H, NC$H_3$), 1.87 (s, 9H, C(C$H_3$)$_3$), 1.35 (s, 9H, C(C$H_3$)$_3$). $^{13}$C{$^1$H} NMR (126 MHz, $C_6D_6$, 283 K): $\delta$ 168.9 (N=*C*H), 158.5 (*C*q), 152.1 (*C*q), 150.4 (*C*q), 149.8 (*C*q), 141.6 (*C*q), 139.5 (*C*q), 134.3 (*C*q), 131.1 (*C*H), 128.8 (*C*H), 128.7 (*C*H), 127.1 (*C*H), 127.0 (*C*H), 125. 8 (*C*H), 124.4 (*C*H), 122.6 (*C*q), 119.8 (*C*H), 119.4 (*C*H), 118.5 (*C*H), 109.1 (*C*H), 71.5 (Zr-*C*H$_2$Ph), 68.0 (Zr-*C*H$_2$Ph), 54.7 (N-*C*H$_2$), 35.7 (*C*(CH$_3$)$_3$), 34.4 (*C*(CH$_3$)$_3$), 31.6 (C(*C*H$_3$)$_3$), 29.8 (C(*C*H$_3$)$_3$), 28.9 (N-*C*H$_3$). IR (KBr (s), $cm^{-1}$): 3061 (m), 3007 (m), 2960 (s), 2908 (m), 2865 (m), 1617 (s), 1588 (s), 1561(m), 1546 (w), 1495 (m), 1478 (s), 1459 (m), 1438 (m), 1422 (m), 1415(m), 1403 (m), 1393 (m), 1362 (w), 1319 (m), 1292 (m), 1277 (m) 1257 (m), 1208 (s), 1177 (m), 1152 (w), 1094 (w), 1055 (w), 1027 (w), 1007 (w), 938 (s), 915 (m), 879 (w), 858 (m), 796 (m), 744 (s), 732 (m), 699 (s), 603 (w), 543 (w), 466 (w).

#### 4.2.5. [NNO]Hf($CH_2Ph$)$_3$ (**7**)

Using an analogous procedure to that described for **6**, reaction of **1** (0.175 g, 0.46 mmol) with $Hf(CH_2Ph)_4$ (0.251 g, 0.46 mmol) afforded **7** as an orange powder. Yield = 0.29 g (76%). Anal. Calc. for $C_{45}H_{51}HfN_3O$ (828.41): C, 65.24; H, 6.21; N, 5.07. Found: C, 65.39; H, 6.14, N 4.97%. $^1$H NMR (400 MHz, $C_6D_6$, 298 K): $\delta$ 7.90 (d, 1H, $^3J_{HH}$ = 2.8 Hz, Ar*H*), 7.49 (d, 2H, $^3J_{HH}$ = 7 Hz, Ar*H*), 7.41 (t, 2H, $^3J_{HH}$ = 7.7 Hz, Ar*H*), 7.31 (t, 1H, $^3J_{HH}$ = 7 Hz, Ar*H*), 7.17 (d, 1H, $^3J_{HH}$ = 8 Hz, Ar*H*), 7.07 (m, 2H, Ar*H* and N=C*H*), 7.03 (d, 1H, $^3J_{HH}$ = 2.4 Hz, Ar*H*), 6.91 (d, 1H, $^3J_{HH}$ = 8 Hz, Ar*H*), 6.85 (d, 1H, $^3J_{HH}$ = 8 Hz, Ar*H*), 6.41 (m, 6H, *meta* + *para*-$CH_2Ph$), 5.84 (d, 4H, $^3J_{HH}$ = 6.8 Hz, *ortho*-$CH_2Ph$), 2.84 (broad s, 2H, Hf-C$H_2$Ph), 2.67 (s, 2H, N-C$H_2$), 2.55 (s, 3H, N-C$H_3$), 2.48 (d, 2H, $^2J_{HH}$ = 9.6 Hz, Hf-CH(*H*)Ph), 2.32 (d, 2H, $^2J_{HH}$ = 9.6 Hz, Hf-C*H*(H)Ph), 1.86 (s, 9H, C(C$H_3$)$_3$), 1.34 (s, 9H, C(C$H_3$)$_3$). $^{13}$C{$^1$H} NMR (101 MHz, $C_6D_6$, 298 K): $\delta$ 169.6 (N=*C*H), 158.3 (*C*q), 152.5 (*C*q), 152.1 (*C*q), 149.5 (*C*q), 142.1 (*C*q), 139.9 (*C*q), 137.6 (*C*q), 134.6 (*C*q), 131.4 (*C*H), 128.8 (*C*H), 128.6 (*C*H), 128.5 (*C*q), 127.5 (*C*H), 126.8 (*C*H), 125.4 (*C*H), 124.9 (*C*H), 124.4 (*C*H), 123.1 (*C*q), 120.1 (*C*H), 119.7 (*C*H), 118.3 (*C*H), 109.9 (*C*H), 77.9 (Hf-$CH_2$Ph), 69.5 (Hf-*C*H$_2$Ph), 54.0 (N-*C*H$_2$), 35.7 (*C*(CH$_3$)$_3$), 34.4 (*C*(CH$_3$)$_3$), 31.6 (C(*C*H$_3$)$_3$), 29.8 (C(CH$_3$)$_3$), 28.9 (N-CH$_3$). IR (KBr (s), $cm^{-1}$): 3063 (m), 3035 (w), 3007 (m), 2954 (s), 2906 (m), 2869 (m), 1617 (s), 1589 (s), 1561 (m), 1506 (m), 1478 (s), 1459 (m), 1441 (m), 1424 (m), 1415 (m), 1403 (m), 1360 (w), 1318 (w), 1289 (m), 1279 (m), 1256 (m), 1241 (w), 1208 (m), 1176 (m), 1057 (w), 1027 (w), 100 (w), 950 (s), 883 (w), 861 (m), 798 (w), 744 (s), 698 (s), 681 (m), 601 (w), 568 (w), 542 (w), 518 (w), 466 (w).

#### 4.2.6. $^{tBu}$[NN(H)O]TiCl$_3$ (**8**)

To a solution of $TiCl_4(THF)_2$ (0,092 g, 0.275 mmol) in THF (10 ml), was added a solution of **2** (0.120 g, 0.275 mmol) in THF (10 mL). The resulting red solution was stirred 2 h at room temperature. The volatiles were removed in vacuo to afford a dark red solid. Crystallisation from hot toluene affords dark red crystals. Yield = 0.12 g (74%). Anal. Calc. for $C_{28}H_{40}Cl_3N_3OTi$ (588.86): C, 57.11; H, 6.85; N, 7.14. Found: C, 57.18; H, 6.75; N, 7.06%. $^1$H NMR (500 MHz, $CDCl_3$, 298 K): $\delta$ 8.60 (d, 1H, $^3J_{HH}$ = 8.1 Hz, Ar*H*), 7.49–7.38 (m, 3H Ar*H*), 7.31 (d, 1H, Ar*H*), 6.89 (d, 1H, Ar*H*), 4.92 (dd (br), 1H, $^3J_{HH}$ = 1.4 Hz, $^3J_{HH}$ = 12.0 Hz, N*H*), 4.71 (t (br), 1H, $^2J_{HH}$ = 12.0 Hz, C(*H*)H), 4.37 (d (br), 1H, $^2J_{HH}$ = 12.0 Hz, C(H)*H*), 3.84 (s, 3H, N-C$H_3$), 3.64 (br d, 1H, $^3J_{HNH}$ = 1.4 Hz, C*H*-$^t$Bu), 1.59 (s, 9H, C(C$H_3$)$_3$), 1.31 (s, 9H, C(C$H_3$)$_3$), 1.07 (s, 9H, C(C$H_3$)$_3$). $^{13}$C{$^1$H} NMR (126 MHz, $CDCl_3$, 298 K): $\delta$ 151.9 (*C*q), 144.5 (*C*q), 137.9 (*C*q), 134.3 (*C*q), 133.5 (*C*q), 126.6 (*C*q), 126.0 (*C*H), 125.2 (*C*H), 122.9 (*C*H), 120.1 (*C*H), 109.5 (*C*H), 75.6 (*C*H-$^t$Bu), 52.4 (*C*H$_2$), 37.7 (*C*(CH$_3$)$_3$), 35.1 (*C*(CH$_3$)$_3$), 34.5 (*C*(CH$_3$)$_3$), 31.4 (C(CH$_3$)$_3$), 31.0 (N-*C*H$_3$), 30.4 (C(*C*H$_3$)$_3$), 27.3 (C(*C*H$_3$)$_3$). IR (KBr (s), $cm^{-1}$): 3265 (w), 3233 (w), 2960 (s), 2910 (m), 2871 (m), 1615 (w), 1595 (w), 1502 (s), 1482 (m), 1459 (s), 1439 (w), 1419 (m), 1365 (m), 1327(w), 1294 (w), 1259 (w), 1235 (s), 1204 (w), 1171 (m), 1109 (w), 1053 (w), 1036 (w), 1012 (w), 932 (w), 913 (w), 875 (m), 861 (w), 785 (w), 761 (m), 750 (s), 643 (w), 600 (m), 475(w), 411 (m).

#### 4.2.7. $^{tBu}$[NNO]Zr($CH_2Ph$)$_2$ (**9**)

Employing an analogous procedure to that described for **6, 2** (0.150 g, 0.34 mmol) was reacted with $Zr(CH_2Ph)_4$ (0.156 g, 0.34 mmol) to give **9** as a white powder. Yield = 0.19 g (78%). Anal. Calc. for $C_{42}H_{53}N_3OZr$ (707.13): C, 71.34; H, 7.55; N, 5.94. Found: C, 71.68; H, 7.23; N 5.87%. $^1$H NMR (500 MHz, $C_6D_6$, 298 K): $\delta$ 7.93 (d, 1H, $^3J_{HH}$ = 8.1 Hz, Ar*H*), 7.53 (m, 3H, Ar*H*), 7.47 (m, 2H, Ar*H*), 7.19 (dt, 1H, Ar*H*), 7.09–7.14 (m, 2H, Ar*H*), 6.71 (d, 1H, $^3J_{HH}$ = 8.0 Hz, Ar*H*), 6.45 (t, 2H, $^3J_{HH}$ = 7.5 Hz, *meta*-$CH_2Ph$), 6.36 (t, 1H, $^3J_{HH}$ = 7.2 Hz, *para*-$CH_2Ph$), 5.74 (d, 2H, $^3J_{HH}$ = 7.2 Hz, *ortho*-$CH_2Ph$), 4.09 (d, 1H, $^2J_{HH}$ = 19.2 Hz, NC(*H*)H), 3.48 (d, 1H, $^2J_{HH}$ = 19.2 Hz, NC(H)*H*), 3.33 (s, 1H, NC*H*$^t$Bu), 2.95 (d, 1H, $^2J_{HH}$ = 9.8 Hz, Zr-C*H*(H) Ph), 2.61 (d, 1H, $^2J_{HH}$ = 9.8 Hz, Zr-CH(*H*)Ph), 2.41 (s, 3H, N-C$H_3$), 2.14 (d, 1H, $^2J_{HH}$ = 10.5 Hz, Zr-C*H*(H)Ph), 1.67 (s, 9H, C(C$H_3$)$_3$), 1.63 (d, 1H, $^2J_{HH}$ = 10.5 Hz, Zr-CH(*H*)Ph), 1.48 (s, 9H, C(C$H_3$)$_3$), 1.19 (s, 9H, C(C$H_3$)$_3$). $^{13}$C{$^1$H} NMR (126 MHz, $C_6D_6$, 298 K): $\delta$ 160.4 (*C*q), 156.1 (*C*q), 149.5 (*C*q), 141.6 (*C*q), 139.7 (*C*q), 139.0 (*C*q), 135.4 (*C*q), 135.2 (*C*q), 132.1 (*C*q), 131.8 (*C*H), 128.3 (*C*H), 127.4 (*C*H), 126.9 (*C*H), 126.3 (*C*H), 124.6 (*C*H), 123.7 (*C*H), 123.6 (*C*H), 123.5 (*C*H), 121.7 (*C*H), 119.2 (*C*H), 118.7 (*C*H), 109.5 (*C*H), 80.8 (NC*H*$^t$Bu), 59.4 (Zr-$CH_2$Ph), 58.8 (Zr-$CH_2$Ph), 56.9 (N-*C*H$_2$), 40.0 (*C*(CH$_3$)$_3$), 35.3 (*C*(CH$_3$)$_3$), 34.4 (*C*(CH$_3$)$_3$), 32.1 (C(*C*H$_3$)$_3$), 30.6 (C(CH$_3$)$_3$), 28.6 (N-CH$_3$), 28.1 (C(CH$_3$)$_3$). IR (KBr (s), $cm^{-1}$): 3062 (w), 3048 (w), 3005 (w), 2954 (s), 2904 (m), 2865 (m), 2787 (w), 1619 (w), 1590 (m), 1494 (m), 1481 (s), 1457 (s), 1443 (m), 1418 (w), 1389 (w), 1361 (m), 1314 (m), 1284 (m), 1248 (s), 1239 (m), 1202 (m), 1169 (m), 1133 (w), 1110 (m), 1068 (m), 1020 (w), 914 (w), 868 (w), 848 (m), 790 (w), 740 (s), 697 (m), 655 (w), 580 (w), 566 (w), 536 (w), 426 (w).

#### 4.2.8. $^{tBu}$[NNO]Hf($CH_2Ph$)$_2$ (**10**)

Employing an analogous procedure to that described for **6, 2** (0.154 g, 0.35 mmol) was reacted with $Hf(CH_2Ph)_4$ (0.192 g, 0.35 mmol) to afford **10** as a white powder. Yield = 0.22 g (77%). Anal. Calc. for $C_{42}H_{53}HfN_3O$ (794.38): C, 63.50; H, 6.72; N, 5.29. Found: C, 63.37; H, 6.80; N 5.24%. $^1$H NMR (400 MHz, $C_6D_6$, 298 K): $\delta$ 7.87 (d, 1H, $^3J_{HH}$ = 7.9 Hz, Ar*H*), 7.56 (d, 3H, $^3J_{HH}$ = 8.3 Hz,

ArH), 7.45 (t, 2H, $^3J_{HH}$ = 7.7 Hz, ArH), 7.20 (m, 1H, ArH), 7.13 (m, 3H, ArH), 6.72 (d, 1H, $^3J_{HH}$ = 7.9 Hz, ArH), 6.48 (t, 2H, $^3J_{HH}$ = 7.2 Hz, *meta*-$CH_2$Ph), 6.37 (t, 1H, $^3J_{HH}$ = 7.2 Hz, *para*-$CH_2$Ph), 5.74 (d, 2H, $^3J_{HH}$ = 7.1 Hz, *ortho*-$CH_2$Ph), 4.25 (d, 1H, $^2J_{HH}$ = 19 Hz, N-C*H*(H)), 3.50 (d, 1H, $^2J_{HH}$ = 19 Hz, N-CH(*H*)), 3.46 (s, 1H, NC*H*$^t$Bu), 2.86 (d, 1H, $^2J_{HH}$ = 11.3 Hz, Hf-C*H*(H) Ph), 2.44(d, 1H, $^2J_{HH}$ = 11.3 Hz, Hf-CH(*H*)Ph), 2.41 (s, 3H, N-$CH_3$), 2.18 (d, 1H, $^2J_{HH}$ = 11.1 Hz, Hf-C*H*(H)Ph), 1.72 (s, 9H, C(C$H_3$)$_3$), 1.55 (d, 1H, $^2J_{HH}$ = 11.1 Hz, Hf-CH(*H*)Ph), 1.49 (s, 9H, C(C$H_3$)$_3$), 1.18 (s, 9H, C(C$H_3$)$_3$)). $^{13}$C{$^1$H} NMR (101 MHz, $C_6D_6$, 298 K): δ 161.0 (*C*q), 156.0 (*C*q), 148.6 (*C*q), 142.1 (*C*q), 139.7 (*C*q), 138.9 (*C*q), 136.3 (*C*q), 135.3 (*C*q), 132.4 (*C*q), 130.7 (*C*H), 128.3 (*C*H), 127.9 (*C*H), 126.8 (*C*H), 126.2 (*C*H), 125.3 (*C*H), 123.9 (*C*H), 123.8 (*C*H), 123.3 (*C*H), 121.8 (*C*H), 119.7 (*C*H), 118.7 (*C*H), 109.6 (*C*H), 80.3 (N*C*H($^t$Bu)), 67.4 (Hf-*C*$H_2$Ph), 65.8 (Hf-$CH_2$Ph), 56.5 (N-*C*$H_2$), 40.0 (*C*(C$H_3$)$_3$), 35.3 (*C*(C$H_3$)$_3$), 34.3 (*C*(C$H_3$)$_3$), 32.1 (C(C$H_3$)$_3$), 30.7 (C(*C*$H_3$)$_3$), 28.5 (N-*C*$H_3$), 28.1 (C(C$H_3$)$_3$). IR (KBr (s), cm$^{-1}$): 3063 (w), 3048 (w), 3006 (w), 2952 (w), 2905 (m), 2863 (m), 2786 (w), 1590 (m), 1531 (w), 1494 (m), 1481 (s), 1456 (s), 1442 (m), 1417 (w), 1388 (w), 1360 (m), 1313(w), 1287 (m), 1250 (s), 1240 (m), 1200 (m),1167 (m), 1133 (w), 1115 (m),1073 (m), 1027 (w), 1006 (w), 975 (w), 936 (w), 869 (w), 848 (m), 791 (m), 742 (s), 704 (m), 657 (w), 648 (w), 581 (w), 570 (w), 536 (w), 480 (w), 428 (w).

#### 4.2.9. $^{Bn}$[NNO]Zr($CH_2$Ph)$_2$ (**11**)

In a glove box, a solution of the pro-ligand **1** (0.169 g, 0.45 mmol) in toluene (5 mL) was added to a solution of Zr($CH_2$Ph)$_4$ (0.204 g, 0.45 mmol) in toluene (5 ml). The resulting solution was stirred at 40 °C overnight and volatiles were removed under reduced pressure. The solid residue was washed with cold pentane, filtered and dried under vacuum to afford a pale pink solid. Yield = 0.28g (86%). Anal. Calc. for $C_{45}H_{51}N_3OZr$ (741.14): C, 72.93; H, 6.94; N, 5.67. Found: C, 72.81; H, 6.81; N 5.48%. $^1$H NMR (500 MHz, $C_6D_6$, 298 K): δ 7.89 (d, 1H, $^3J_{HH}$ = 8.1 Hz, Ar*H*), 7.54 (d, 1H, $^4J_{HH}$ = 2.4 Hz, Ar*H*), 7.48 (m, 4H, Ar*H*), 7.19 (dt, 1H, $^3J_{HH}$ = 8.1 Hz, Ar*H*), 7.00–7.12 (m, 7H, Ar*H*), 6.94 (d, 1H, $^4J_{HH}$ = 2.4 Hz, Ar*H*), 6.64 (d, 1H, $^3J_{HH}$ = 8.1 Hz, Ar*H*), 6.46 (t, 2H, $^3J_{HH}$ = 7.6 Hz, *meta*-$CH_2$Ph), 6.34 (t, 1H, $^3J_{HH}$ = 7.2 Hz, *para*-$CH_2$Ph), 6.09 (d, 2H, $^3J_{HH}$ = 7.2 Hz, *ortho*-$CH_2$Ph), 3.89 (t, 1H, $^3J_{HH}$ = 6.9 Hz, C*H*-$CH_2$Ph), 3.70 (q, 2H, $^2J_{HH}$ = 18.8 Hz, N-C$H_2$), 3.30 (m, 2H, $^2J_{HH}$ = 12.7 Hz, $^3J_{HH}$ = 6.9 Hz, CH-C$H_2$Ph), 2.79 (d, 1H, $^2J_{HH}$ = 9.4 Hz, Zr-C*H*(H)Ph), 2.59 (d, 1H, $^2J_{HH}$ = 9.4 Hz, Zr-CH(*H*) Ph), 2.28 (s, 3H, N-C$H_3$), 2.10 (d, 1H, $^2J_{HH}$ = 10.7 Hz, Zr-C*H*(H)Ph), 1.79 (s, 9H, C(C$H_3$)$_3$), 1.64 (d, 1H, $^2J_{HH}$ = 10.7 Hz, Zr-CH(*H*)Ph), 1.39 (s, 9H, C(C$H_3$)$_3$). $^{13}$C{$^1$H} NMR (126 MHz, $C_6D_6$, 298 K): δ 160.7 (*C*q), 155.5 (*C*q), 149.2 (*C*q), 141.6 (*C*q), 141.0 (*C*q), 140.7 (*C*q), 138.8 (*C*q), 135.7 (*C*q), 135.0 (*C*q), 134.3 (*C*q), 131.9 (*C*H), 130.0 (*C*H), 128.2 (*C*H), 127.4 (*C*H), 127.2 (*C*H), 125.9 (*C*H), 125.0 (*C*H), 123.8 (*C*H), 123.7 (*C*H), 123.5 (*C*H), 123.2 (*C*H), 122.0 (*C*H), 119.5 (*C*H), 119.1 (*C*H), 109.5 (*C*H), 73.6 (*C*H-$CH_2$Ph), 58.9 (Zr-$CH_2$Ph), 57.7 (Zr-$CH_2$Ph), 55.0 (N-$CH_2$), 48.9 (CH-$CH_2$PH), 35.5 (*C*(C$H_3$)$_3$), 34.4 (*C*(C$H_3$)$_3$), 32.0 (C(C$H_3$)$_3$), 30.8 (C(*C*$H_3$)$_3$), 28.6 (N-$CH_3$). IR (KBr (s), cm$^{-1}$): 3054 (w), 3020 (w), 2951 (s), 2904 (m), 2858 (m), 1617 (w), 1600 (w), 1589 (w), 1495 (m), 1480 (s), 1457 (s), 1440 (s), 1418 (m), 1390 (w), 1359 (m), 1289 (m), 1260 (m), 1237 (m), 1203 (w), 1176 (w), 1128 (w), 1099 (w), 1078 (m), 1027 (w), 1008 (w), 929 (w), 876 (w), 845 (w), 799 (w), 740 (s), 698 (m), 532 (m), 463 (w), 449 (w).

#### 4.2.10. $^{Bn}$[NNO]Hf($CH_2$Ph)$_2$ (**12**)

Employing an analogous procedure to that described for **11**, **1** (0.168 g, 0.45 mmol) was reacted with Hf($CH_2$Ph)$_4$ (0.241 g, 0,44 mmol) at 50 °C for 24 h to give a pale pink solid. Yield = 0.33g (90%). Anal. Calc. for $C_{45}H_{51}HfN_3O$ (828.41): C, 65.24; H, 6.21; N, 5.07. Found: C 65.43, H 6.14, N, 5.03%. $^1$H NMR (500 MHz, $C_6D_6$, 298 K): δ 7.81 (d, 1H, $^3J_{HH}$ = 8.1 Hz, Ar*H*), 7.56 (d, 1H, $^4J_{HH}$ = 2.4 Hz, Ar*H*), 7.47 (d, 2H, $^3J_{HH}$ = 7.1 Hz, Ar*H*), 7.40 (t, 2H, $^3J_{HH}$ = 7.7 Hz, Ar*H*), 7.00–7.07 (m, 7H, Ar*H*), 6.89 (d, 1H, $^4J_{HH}$ = 2.2 Hz, Ar*H*), 6.64 (d, 1H, $^3J_{HH}$ = 8.1 Hz, Ar*H*), 6.55 (t, 2H, $^3J_{HH}$ = 7.6 Hz, *meta*-$CH_2$Ph), 6.40 (t, 1H, $^3J_{HH}$ = 7.2 Hz, *para*-$CH_2$Ph), 6.18 (d, 2H, $^3J_{HH}$ = 7.5 Hz, *ortho*-$CH_2$Ph), 4.02 (t, 1H, $^3J_{HH}$ = 6.7 Hz, C*H*-$CH_2$Ph), 3.77 (q, 2H, $^2J_{HH}$ = 18.6 Hz, N-C$H_2$), 3.21 (m, 2H, $^2J_{HH}$ = 12.7 Hz, $^3J_{HH}$ = 6.8 Hz, CH-C$H_2$Ph), 2.62 (d, 1H, $^2J_{HH}$ = 10.9 Hz, Hf-C*H*(H)Ph), 2.46 (d, 1H, $^2J_{HH}$ = 10.9 Hz, Hf-CH(*H*)Ph), 2.26 (s, 3H, N-C$H_3$), 2.16 (d, 1H, $^2J_{HH}$ = 11.5 Hz, Hf-C*H*(H)Ph), 1.83 (s, 9H, C(C$H_3$)$_3$), 1.67 (d, 1H, $^2J_{HH}$ = 11.5 Hz, Hf-CH(*H*)Ph), 1.38 (s, 9H, C(C$H_3$)$_3$). $^{13}$C{$^1$H} NMR (126 MHz, $C_6D_6$, 298 K): δ 161.3 (*C*q), 155.3 (*C*q), 148.3 (*C*q), 142.4 (*C*q), 141.0 (*C*q), 140.7 (*C*q), 138.8 (*C*q), 136.6 (*C*q), 135.1 (*C*q), 134.4 (*C*q), 130.5 (*C*H), 129.9 (*C*H), 128.5 (*C*H), 127.8 (*C*H), 127.3 (*C*H), 125.8 (*C*H), 124.0 (*C*H), 123.8 (*C*H), 123.7 (*C*H), 123.0 (*C*H), 122.2 (*C*H), 120.1 (*C*H), 119.0 (*C*H), 109.5 (*C*H), 73.1 (*C*H-$CH_2$Ph), 66.9 (Hf-*C*$H_2$Ph), 66.2 (Hf-*C*$H_2$Ph), 54.6 (N-*C*$H_2$), 48.2 (CH-*C*$H_2$Ph), 35.6 (*C*(C$H_3$)$_3$), 34.4 (*C*(C$H_3$)$_3$), 32.0 (C(*C*$H_3$)$_3$), 30.8 (C(*C*$H_3$)$_3$), 28.6 (N-$CH_3$). IR (KBr (s), cm$^{-1}$): 3054 (w), 3020 (w), 2951 (s), 2899 (m), 2858 (m), 2801 (w), 2772 (w), 1589 (m), 1497 (m), 1477 (s), 1457 (s), 1442 (m), 1414 (w), 1356 (w), 1316 (w), 1284 (m), 1253 (s), 1238 (m), 1201 (m), 1178 (m), 1126 (w), 1118 (w), 1083 (m), 1026 (w), 1006 (w), 971 (w), 931 (w), 873 (w), 850 (m), 805 (w), 787 (w), 773 (w), 741 (s), 695 (m), 606 (w), 566 (w), 529 (w), 431 (w).

#### 4.2.11. $^{Bn}$[NNO]Ti($CH_2$Ph)$_2$ (**13**)

To a solution of **3** (0.21 g, 0.39 mmol) in THF (20 mL) at −78 °C was added 0.9 mL (1.18 mmol) of a $PhCH_2MgCl$ solution (20 wt%) in THF. The reaction was stirred for 3 h at −78 °C, filtered and the volatiles then evaporated under vacuum keeping the temperature below 0 °C, to afford a brown-red solid. The solid was washed with cold pentane, filtered and dried under vacuum. Yield = 0.12g (44%). Satisfactory elemental analysis could not be obtained due to the thermal sensitivity of the sample. $^1$H NMR (400 MHz, $C_6D_6$, 298 K): δ 7.94 (d, 1H, $^3J_{HH}$ = 7.9 Hz, Ar*H*), 7.54 (d, 1H, $^4J_{HH}$ = 2.4 Hz, Ar*H*), 7.40 (d, 2H, $^3J_{HH}$ = 7.2 Hz, Ar*H*), 7.22 (t, 2H, $^3J_{HH}$ = 7.5 Hz, Ar*H*), 7.00 (m, 7H, ArH), 6.81 (d, 1H, $^4J_{HH}$ = 2.4 Hz, Ar*H*), 6.74 (d, 1H, $^3J_{HH}$ = 7.9 Hz, Ar*H*), 6.50 (t, 2H, $^3J_{HH}$ = 7.4 Hz, *meta*-$CH_2$Ph), 6.40 (t, 1H, $^3J_{HH}$ = 7.2 Hz, *para*-$CH_2$Ph), 6.01 (d, 2H, $^3J_{HH}$ = 7.3 Hz, *ortho*-$CH_2$Ph), 3.79 (t, 1H, $^3J_{HH}$ = 6.9 Hz, C*H*-$CH_2$Ph), 3.64 (q, 2H, $^2J_{HH}$ = 19.4 Hz, N-C$H_2$), 3.28 (d, 1H, $^2J_{HH}$ = 9.2 Hz, Ti-CH(*H*)Ph), 3.22 (d, 1H, $^2J_{HH}$ = 9.2 Hz, Ti-C*H*(H)Ph), 2.97 (m, 2H, $^2J_{HH}$ = 12.8 Hz, $^3J_{HH}$ = 6.9 Hz, CH-C$H_2$Ph), 2.57 (d, 1H, $^2J_{HH}$ = 9 Hz, Ti-CH(*H*)Ph), 2.39 (d, 1H, $^2J_{HH}$ = 9 Hz, Ti-C*H*(H)Ph), 2.38 (s, 3H, N-C$H_3$), 1.91 (s, 9H, C(C$H_3$)$_3$), 1.34 (s, 9H, C(C$H_3$)$_3$). $^{13}$C{$^1$H} NMR (101 MHz, $C_6D_6$, 298 K): δ 162.9 (*C*q), 157.4 (*C*q), 152.6 (*C*q), 149.6 (*C*q), 141.7 (*C*q), 141.1 (*C*q), 137.0 (*C*q), 136.1 (*C*q), 135.0 (*C*q), 134.8 (*C*q), 129.8 (*C*H), 129.1 (*C*H), 128.8 (*C*H), 126.7 (*C*H), 126.0 (*C*H), 125.5 (CH), 125.0 (CH), 123.5 (*C*H), 123.2 (*C*H), 123.0 (CH), 122.0 (*C*H), 121.8 (CH), 120.3 (*C*H), 119.0 (*C*H), 109.4 (*C*H), 75.9 (Ti-$CH_2$Ph), 74.8 (Ti-$CH_2$Ph), 64.8 (*C*H-$CH_2$Ph), 56.2 (N-*C*$H_2$), 37.8 (CH-$CH_2$Ph), 35.6 (*C*(C$H_3$)$_3$), 34.2 (*C*(C$H_3$)$_3$), 31.7 (C(C$H_3$)$_3$), 31.0 (C(*C*$H_3$)$_3$), 28.5 (N-$CH_3$).

#### 4.2.12. {[NNO]Ti($NMe_2$)$_2$}$_2$ (**14**)

A solution of **1** (0.347 g, 0.92 mmol) in toluene (4 mL) was added to a solution of Ti($NMe_2$)$_4$ (0.206 g, 0.92 mmol) in toluene (2 mL). The resulting dark brown solution was stirred for 30 min at room temperature and allowed to stand overnight. An orange crystalline solid precipitated out of the solution and was isolated by filtration and dried under vacuum. Yield = 0.32 g (68% in respect to **1**). Anal. Calc. for $C_{56}H_{82}N_{10}O_2Ti_2$ (1022.56): C, 65.74; H, 8.08; N, 13.69. Found: C, 65.61; H, 7.92; N, 13.58%. $^1$H NMR (400 MHz, THF-$d_8$, 298 K): δ 7.70 (d, 2H, Ar*H*, $^3J_{HH}$ = 7.5 Hz), 7.23–7.30 (m, 6H, Ar*H*), 7.16 (d, 2H, Ar*H*, $^4J_{HH}$ = 2.4 Hz), 6.18 (d, 2H, Ar*H*, $^4J_{HH}$ = 2.4 Hz), 4.50 (d, 2H, C*H*, $^3J_{HH}$ = 7.3 Hz), 4.00 (d, 2H, C*H*, $^3J_{HH}$ = 7.3 Hz), 3.49 (s,

12H, Ti-N($CH_3$)$_2$), 2.89 (s, 12H, Ti-N($CH_3$)$_2$), 2.78 (s, 6H, N-$CH_3$), 1.58 (s, 9H, C($CH_3$)$_3$), 0.84 (s, 18H, C($CH_3$)$_3$). $^{13}$C{1H} NMR (101 MHz, THF-$d_8$, 298 K): δ 160.6 (*C*q), 159.5 (*C*q), 135.6 (*C*q), 135.1 (*C*q), 129.65 (*C*q), 128.74 (*C*q), 123.5 (Ar*C*H), 122.9 (*C*q), 122.7 (Ar*C*H), 122.1 (Ar*C*H), 117.9 (Ar*C*H), 110.1 (Ar*C*H), 84.4 (*C*H), 72.1 (*C*H), 46.0 (Ti-N($CH_3$)$_2$), 35.0 (*C*($CH_3$)$_3$), 33.5 (*C*($CH_3$)$_3$), 31.0 (C(*C*H$_3$)$_3$), 29.3 (C(*C*H$_3$)$_3$), 28.8 (N-*C*H$_3$). IR (KBr (s), cm$^{-1}$): 2952 (s), 2905 (m), 2860 (m), 2813 (m), 2765 (m), 1617 (w), 1523 (w), 1494 (m), 1475 (s), 1459 (s), 1442 (s), 1416 (m), 1360 (w), 1333 (w), 1271 (s), 1258 (m), 1202 (w), 1171 (w), 1132 (w), 1101 (w), 1062 (w), 1004 (w), 942 (s), 926 (m), 877 (w), 841 (m), 790 (m), 743 (s), 699 (w), 650 (w), 590 (w) 565 (m), 549 (m), 489 (w), 482 (w).

#### 4.2.13. 2-aminomethyl-1-methylbenzimidazole dihydrochloride-$d_2$

*N*-Methylphenylenediamine (5 g, 41 mmol) and glycine-2-$d_2$ ethyl ester hydrochloride (5.8 g, 41 mmol) were refluxed in HCl 6 M (100 mL). After cooling, the blue solution was boiled with charcoal, filtered and volatiles were evaporated to afford dark blue oil. Trituration in absolute ethanol afforded a blue crystalline product. Yield = 4.8 g (50%), Anal. Calc. for $C_9H_9D_2N_3 \cdot 2HCl$ (236.14): C, 45.78; H, 4.70; N, 17.79. Found: C, 45.83; H, 4.79; N, 17.68%. $^1$H NMR (400 MHz, $D_2O$, 298 K): $\delta$ 7.84 (m, 2H, Ar*H*), 7.66 (m, 2H, Ar*H*), 4.09 (s, 3H, N-$CH_3$). $^{13}$C NMR (101 MHz, $D_2O$, 298 K): δ 143.5 (*C*q), 132.7 (*C*q), 130.4 (*C*q), 127.5 (*C*H), 127.1 (*C*H), 114.6 (*C*H), 112.8 (*C*H), 32.5 (*C*D$_2$), 31.6 (N-*C*H$_3$). MS (positive ES; *m*/*z*): 164 [M−2HCl]$^+$.

#### 4.2.14. $d_2$-NNO (**1d$_2$**)

Following similar procedure described for **1**, using 2-aminomethyl-1-methylbenzimidazole dihydrochloride-$d_2$ (1.95 g, 8.26 mmol), potassium carbonate (1.14 g, 8.26 mmol) and 3,5-di-*tert*-butyl-salicylaldehyde (1.95 g, 8.26 mmol). Yield = 1.8 g (60%), Anal. Calc. for $C_{24}H_{29}D_2N_3O$ (379.53): C, 75.95; H, 7.70; N, 11.07. Found: C, 75.81; H, 7.80; N, 10.97%. $^1$H NMR (400 MHz, $CDCl_3$, 298 K): $\delta$ 13.13 (s, 1H, O*H*), 8.54 (t, 1H, N=C*H*), 7.76 (d, 1H, Ar*H*), 7.39 (d, 1H, Ar-*H*, $^4J_{HH}$ = 2.5 Hz), 7.37 (m, 1H, Ar*H*), 7.31 (m, 2H, Ar*H*), 7.08 (d, 1H, Ar-*H*, $^4J_{HH}$ = 2.5 Hz), 3.91 (s, 3H, N-*C*H$_3$), 1.41 (s, 9H, C(*C*H$_3$)$_3$), 1.28 (s, 9H, C(*C*H$_3$)$_3$). $^{13}$C{$^1$H} NMR (101 MHz, $CDCl_3$, 298 K): δ 169.1 (N=*C*H), 157.7 (*C*q), 150.7 (*C*q), 142.3 (*C*q), 140.5 (*C*q), 136.7 (*C*q), 136.2 (*C*q), 127.7 (Ar*C*H), 126.5 (Ar*C*H), 122.9 (Ar*C*H), 122.3 (Ar*C*H), 119.9 (Ar*C*H), 117.7 (*C*q), 109.4 (Ar*C*H), 55.5 (*C*D$_2$), 35.00 (*C*(CH$_3$)$_3$), 34.1 (*C*(CH$_3$)$_3$), 31.4 (C(*C*H$_3$)), 30.4 (N-*C*H$_3$), 29.3 (C(*C*H$_3$)). MS (positive ES; *m*/*z*): 380 [M−H]$^+$. IR (KBr (s), cm$^{-1}$): 2997 (w), 2956 (s), 2911 (m), 2869 (m), 2362 (m), 2342 (m), 1626 (s), 1594 (m), 1504 (w), 1469 (s), 1441 (s), 1395 (m), 1377 (w), 1361 (m), 1329 (m), 1285 (w), 1271 (m), 1251 (s), 1202 (s), 1175 (m), 1151 (w), 1131 (w), 1087 (w), 1066 (w), 1027 (w), 1010 (w), 964 (w), 925 (w), 891 (w), 828 (m), 802 (w), 773 (w), 752 (w), 739 (s), 669 (w), 645 (w), 512 (w).

#### 4.2.15. {[$d_2$-NNO]Ti(NMe$_2$)}$_2$ (**14d$_2$**)

In a glove box, **1d$_2$** (0.020 g, 0.053 mmol) and Ti(NMe$_2$)$_4$ (0.012 g, 0.053 mmol) were mixed in $C_6D_6$, the resulting brown solution was stirred for 30 min and allowed to stand overnight, the crystalline precipitate was filtered off, dried and dissolved in THF-$d_8$. $^1$H NMR (400 MHz, THF-$d_8$, 298 K): $\delta$ 7.70 (d, 2H, Ar*H*, $^3J_{HH}$ = 7.5 Hz), 7.23–7.30 (m, 6H, Ar*H*), 7.16 (d, 2H, Ar*H*, $^4J_{HH}$ = 2.4 Hz), 6.18 (d, 2H, Ar*H*, $^4J_{HH}$ = 2.4 Hz), 4.00 (s, 2H, C*H*), 3.49 (s, 12H, Ti-N($CH_3$)$_2$), 2.89 (s, 12H, Ti-N(C$H_3$)$_2$), 2.78 (s, 6H, N-C$H_3$), 1.58 (s, 9H, C($CH_3$)$_3$), 0.84 (s, 18H, C($CH_3$)$_3$). $^{13}$C{1H} NMR (101 MHz, THF-$d_8$, 298 K): δ 160.6 (*C*q), 159.5 (*C*q), 135.6 (*C*q), 135.1 (*C*q), 129.65 (*C*q), 128.74 (*C*q), 123.5 (Ar*C*H), 122.9 (*C*q), 122.7 (Ar*C*H), 122.1 (Ar*C*H), 117.9 (Ar*C*H), 110.1 (Ar*C*H), 84.4

**Table 8**
Crystal data, data collection and refinement parameters for compounds **3, 8, 10, 14, 15** and **16**.[a]

| Data | 3 | 8 | 10 | 14 | 15 | 16 |
|---|---|---|---|---|---|---|
| Formula | $C_{24}H_{30}Cl_3N_3OTi$ | $C_{28}H_{40}Cl_3N_3OTi$ | $C_{42}H_{53}HfN_3O$ | $C_{52}H_{70}Cl_2N_8O_2Ti_2$ | $C_{76}H_{86}N_6O_2Zr_2$ | $C_{76}H_{86}Hf_2N_6O_2$ |
| Solvent | MeCN | $C_7H_8$ | – | $4CH_2Cl_2$ | $4C_6H_6$ | $4C_6H_6$ |
| Formula weight | 571.81 | 681.01 | 794.36 | 1345.56 | 1610.38 | 1784.92 |
| Colour, habit | Red plates | Orange platy needles | Colourless plates | Orange/red blocky needles | Colourless needles | Colourless blocks |
| Crystal size (mm) | 0.14 × 0.09 × 0.02 | 0.42 × 0.24 × 0.04 | | 0.17 × 0.09 × 0.02 | | |
| | 0.29 × 0.13 × 0.07 | 0.41 × 0.18 × 0.12 | | 0.14 × 0.06 × 0.04 | | |
| Temperature (K) | 173 | 173 | 173 | 173 | 173 | 173 |
| Crystal system | Monoclinic | Monoclinic | Monoclinic | Triclinic | Monoclinic | Monoclinic |
| Space group | *Pn* (no. 7) | $P2_1/c$ (no. 14) | $P2_1/c$ (no. 14) | $P\bar{1}$ (no. 2) | $P2_1/n$ (no. 14) | $P2_1/n$ (no. 14) |
| *a* (Å) | 11.19494(19) | 20.4913(5) | 37.4537(4) | 10.5096(8) | 11.76130(6) | 11.76313(10) |
| *b* (Å) | 20.2370(3) | 10.8508(2) | 11.71132(11) | 12.1591(17) | 17.88338(9) | 17.86777(14) |
| *c* (Å) | 25.4362(4) | 16.6923(3) | 17.24202(14) | 13.562(2) | 20.29847(10) | 20.30114(19) |
| α (°) | – | – | – | 98.227(12) | – | – |
| β (°) | 102.4417(16) | 103.126(2) | 91.3951(9) | 94.670(9) | 94.1037(4) | 93.6476(8) |
| γ (°) | – | – | – | 104.768(9) | – | – |
| *V* (Å$^3$) | 5627.3(2) | 3614.51(13) | 7560.64(11) | 1645.9(4) | 4258.47(15) | 4258.27(12) |
| *Z* | 8[b] | 4 | 8[c] | 1[d] | 2[d] | 2[d] |
| $D_c$ (g cm$^{-3}$) | 1.350 | 1.251 | 1.396 | 1.358 | 1.256 | 1.392 |
| Radiation used | Mo Kα | Cu Kα | Cu Kα | Mo Kα | Cu Kα | Mo Kα |
| μ (mm$^{-1}$) | 0.615 | 4.274 | 5.358 | 0.694 | 2.410 | 2.489 |
| 2θ max (°) | 56 | 126 | 126 | 64 | 143 | 65 |
| No. of unique reflections measured | 19976 | 5688 | 11908 | 10256 | 8228 | 14172 |
| Observed, $\|F_o\| > 4\sigma(\|F_o\|)$ | 16983 | 2265 | 8651 | 5894 | 6163 | 10774 |
| No. of variables | 1298 | 365 | 849 | 439 | 498 | 498 |
| $R_1$, $wR_2$[e] | 0.039, 0.091 | 0.045, 0.062 | 0.028, 0.051 | 0.059, 0.141 | 0.026, 0.061 | 0.025, 0.055 |

[a] Details in common: graphite monochromated radiation, refinement based on $F^2$.
[b] There are four independent complexes.
[c] There are two independent complexes.
[d] The complex has crystallographic $C_i$ symmetry.
[e] $R_1 = \sum ||F_o| - |F_c|| / \sum |F_o|$; $wR_2 = \sum [w(F_o^2 - F_c^2)^2] / \sum [w(F_o^2)^2]^{1/2}$; $w^{-1} = \sigma^2(F_o^2) + (aP)^2 + bP$.

(CH), 72.1 (CD), 46.0 (Ti-N($CH_3$)$_2$), 35.0 ($C(CH_3)_3$), 33.5 ($C(CH_3)_3$), 31.0 ($C(CH_3)_3$), 29.3 ($C(CH_3)_3$), 28.8 (N-$CH_3$). IR (KBr (s), $cm^{-1}$): 2953 (s), 2904 (m), 2861 (m), 2812 (m), 2766 (m), 1613 (w), 1492 (m), 1477 (s), 1457 (s), 1443 (s), 1414 (m), 1391 (w), 1360 (w), 1328 (w), 1274 (m), 1250 (m), 1205 (w), 1174 (w), 1174 (w), 1133 (w), 1114 (w), 1057 (w), 1007 (w), 943 (s), 880 (w), 842 (m), 785 (m), 747 (s), 650 (w), 565 (m), 551 (m), 494 (w), 474 (w).

### 4.3. X-ray crystallography

Table 8 provides a summary of the crystallographic data for compounds **3, 8, 10, 14, 15** and **16**. Data were collected using Oxford Diffraction PX Ultra (**8, 10** and **15**) and Xcalibur 3 (**3, 14** and **16**) diffractometers, and the structures were refined based on $F^2$ using the SHELXTL and SHELX-97 program systems [64].

## Acknowledgements

We thank Dr. Stefan Spitzmesser for useful discussions. Ineos Technologies is thanked for financial support and Aurelie Peters for GPC analyses.

## Appendix A. Supplementary material

CCDC 683004, 683005, 683006, 683007, 683008 and 683009 contain the supplementary crystallographic data for **3**, **8**, **10**, **14**, **15** and **16**. These data can be obtained free of charge from The Cambridge Crystallographic Data Centre via www.ccdc.cam.ac.uk/data_request/cif. Supplementary data associated with this article can be found, in the online version, at doi:10.1016/j.jorganchem.2008.11.064.

## References

[1] G.J.P. Britovsek, V.C. Gibson, D.F. Wass, Angew. Chem., Int. Ed. 38 (1999) 428.
[2] V.C. Gibson, S.K. Spitzmesser, Chem. Rev. 103 (2003) 283.
[3] C. Wang, S. Friedrich, T.R. Younkin, R.T. Li, R.H. Grubbs, D.A. Bansleben, M.W. Day, Organometallics 17 (1998) 3149.
[4] S. Matsui, Y. Tohi, M. Mitani, J. Saito, H. Makio, H. Tanaka, M. Nitabaru, T. Nakano, T. Fujita, Chem. Lett. (1999) 1065.
[5] S. Matsui, M. Mitani, J. Saito, Y. Tohi, H. Makio, H. Tanaka, T. Fujita, Chem. Lett. (1999) 1263.
[6] M. Mitani, J. Saito, S.-I. Ishii, Y. Nakayama, H. Makio, N. Matsukawa, S. Matsui, J.-I. Mohri, R. Furuyama, H. Terao, H. Bando, H. Tanaka, T. Fujita, Chem. Record 4 (2004) 137.
[7] Y. Nakayama, H. Bando, Y. Sonobe, T. Fujita, Bull. Chem. Soc. Jpn. 77 (2004) 617.
[8] H. Makio, T. Fujita, Bull. Chem. Soc. Jpn. 78 (2005) 52.
[9] A. Sakuma, M.-S. Weiser, T. Fujita, Polym. J. (Tokyo, Jpn.) 39 (2007) 193.
[10] J. Tian, G.W. Coates, Angew. Chem., Int. Ed. 39 (2000) 3626.
[11] J. Tian, P.D. Hustad, G.W. Coates, J. Am. Chem. Soc. 123 (2001) 5134.
[12] D.A. Pennington, W. Clegg, S.J. Coles, R.W. Harrington, M.B. Hursthouse, D.L. Hughes, M.E. Light, M. Schormann, M. Bochmann, S.J. Lancaster, Dalton Trans. (2005) 561.
[13] D.A. Pennington, D.L. Hughes, M. Bochmann, S.J. Lancaster, Dalton Trans. (2003) 3480.
[14] W.-Q. Hu, X.-L. Sun, C. Wang, Y. Gao, Y. Tang, L.-P. Shi, W. Xia, J. Sun, H.-L. Dai, X.-Q. Li, X.-L. Yao, X.-R. Wang, Organometallics 23 (2004) 1684.
[15] C. Wang, Z. Ma, X.-L. Sun, Y. Gao, Y.-H. Guo, Y. Tang, L.-P. Shi, Organometallics 25 (2006) 3259.
[16] C. Wang, X.-L. Sun, Y.-H. Guo, Y. Gao, B. Liu, Z. Ma, W. Xia, L.-P. Shi, Y. Tang, Macromol. Rapid Commun. 26 (2005) 1609.
[17] G. Paolucci, A. Zanella, L. Sperni, V. Bertolasi, M. Mazzeo, C. Pellecchia, J. Mol. Catal. A: Chem. 258 (2006) 275.
[18] R.K.J. Bott, M. Hammond, P.N. Horton, S.J. Lancaster, M. Bochmann, P. Scott, Dalton Trans. (2005) 3611.
[19] P.D. Knight, A.J. Clarke, B.S. Kimberley, R.A. Jackson, P. Scott, Chem. Commun. (2002) 352.
[20] G.J. Clarkson, V.C. Gibson, P.K.Y. Goh, M.L. Hammond, P.D. Knight, P. Scott, T.M. Smit, A.J.P. White, D.J. Williams, Dalton Trans. (2006) 5484.
[21] K.V. Axenov, M. Klinga, O. Lehtonen, H.T. Koskela, M. Leskelae, T. Repo, Organometallics 26 (2007) 1444.
[22] R.K.J. Bott, D.L. Hughes, M. Schormann, M. Bochmann, S.J. Lancaster, J. Organomet. Chem. 665 (2003) 135.
[23] D.A. Pennington, S.J. Coles, M.B. Hursthouse, M. Bochmann, S. Lancaster, J. Chem. Commun. (2005) 3150.
[24] S.R. Coles, G.J. Clarkson, A.L. Gott, I.J. Munslow, S.K. Spitzmesser, P. Scott, Organometallics 25 (2006) 6019.
[25] M. Sanz, T. Cuenca, M. Galakhov, A. Grassi, R.K.J. Bott, D.L. Hughes, S.J. Lancaster, M. Bochmann, Organometallics 23 (2004) 5324.
[26] D.C.H. Oakes, B.S. Kimberley, V.C. Gibson, D.J. Jones, A.J.P. White, D.J. Williams, Chem. Commun. (2004) 2174.
[27] D.C.H. Oakes, V.C. Gibson, A.J.P. White, D.J. Williams, Inorg. Chem. 45 (2006) 3476.
[28] D.J. Jones, V.C. Gibson, S.M. Green, P.J. Maddox, Chem. Commun. (2002) 1038.
[29] D.J. Jones, V.C. Gibson, S.M. Green, P.J. Maddox, A.J.P. White, D.J. Williams, J. Am. Chem. Soc. 127 (2005) 11037.
[30] A.K. Tomov, V.C. Gibson, D. Zaher, M.R.J. Elsegood, S.H. Dale, Chem. Commun. (2004) 1956.
[31] A.K. Tomov, J.J. Chirinos, R.J. Long, V.C. Gibson, M.R.J. Elsegood, J. Am. Chem. Soc. 128 (2006) 7704.
[34] M.R. Maurya, A. Kumar, M. Ebel, D. Rehder, Inorg. Chem. 45 (2006) 5924.
[35] The maximum deviations from planarity are ca. 0.11, 0.12, 0.14 and 0.15 Å for C(16), C(5), C(9) and C(5) in complexes **3-A**, **3-B**, **3-C** and **3-D**, respectively.
[36] S.L. Latesky, A.K. McMullen, G.P. Niccolai, I.P. Rothwell, J.C. Huffman, Organometallics 4 (1985) 902.
[37] R.F. Jordan, R.E. LaPointe, C.S. Bajgur, S.F. Echols, R. Willett, J. Am. Chem. Soc. 109 (1987) 4111.
[38] R.F. Jordan, R.E. LaPointe, N. Baenziger, G.D. Hinch, Organometallics 9 (1990) 1539.
[39] M. Bochmann, S.J. Lancaster, Organometallics 12 (1993) 633–640.
[40] M. Bochmann, S.J. Lancaster, M.B. Hursthouse, K.M.A. Malik, Organometallics 13 (1994) 2235.
[41] The $\tau$ parameter is defined as $\tau = (b - a)/60°$, where $b$ and $a$ are the largest and second largest angles at the metal centre, respectively (see J. Chem. Soc., Dalton Trans, 1984, 1349–1356 (specifically p. 1352)). For a perfect square-based pyramid, $\tau = 0$ [as $a = b = 180°$], and for a perfect trigonal bipyramid $\tau = 1$ [as $a = 120°$ and $b = 180°$].
[42] For both complexes **10-A** and **10-B** the closest intramolecular approach to the centroid of the C(51) phenyl ring is from a methyl proton on the *t*-butyl group ortho to the oxygen on the C(13)/C(18) aromatic C6 ring, though different methyl groups are involved in each case. For complex **10-A**, a proton on C(29) approaches the centroid with an H$\cdots\pi$ separation of ca. 3.13 Å, whilst for complex **10-B** a proton on C(31′) is ca. 3.30 Å distant. The closest intermolecular approach to the centroid of the C(51) phenyl ring in complex **10-A** is from an N(11)–Me proton of a symmetry related counterpart with an H$\cdots\pi$ separation of ca. 3.34 Å, whilst for complex **10-B** the closest intermolecular approach is from a methylene proton on C(2′) in a symmetry related counterpart with an H$\cdots\pi$ separation of ca. 3.56 Å.
[43] L. Giannini, E. Solari, S. De Angelis, T.R. Ward, C. Floriani, A. Chiesi-Villa, C. Rizzoli, J. Am. Chem. Soc. 117 (1995) 5801.
[44] P.R. Woodman, N.W. Alcock, I.J. Munslow, C.J. Sanders, P. Scott, J. Chem. Soc., Dalton Trans. (2000) 3340.
[45] P.D. Knight, P.N. O'Shaughnessy, I.J. Munslow, B.S. Kimberley, P. Scott, J. Organomet. Chem. 683 (2003) 103.
[46] P.D. Knight, G. Clarkson, M.L. Hammond, B.S. Kimberley, P. Scott, J. Organomet. Chem. 690 (2005) 5125.
[47] H. Tsurugi, T. Yamagata, K. Tani, K. Mashima, Chem. Lett. 32 (2003) 756.
[48] H. Tsurugi, Y. Matsuo, T. Yamagata, K. Mashima, Organometallics 23 (2004) 2797.
[49] P. De Waele, B.A. Jazdzewski, J. Klosin, R.E. Murray, C.N. Theriault, P.C. Vosejpka, J.L. Petersen, Organometallics 26 (2007) 3896.
[50] K. Mashima, R. Ohnishi, T. Yamagata, H. Tsurugi, Chem. Lett. 36 (2007) 1420.
[51] S.J. Trepanier, S. Wang, Can. J. Chem. 74 (1996) 2032.
[52] M. Westerhausen, T. Bollwein, P. Mayer, H. Piotrowski, A.Z. Pfitzner, Anorg. Allg. Chem. 628 (2002) 1425.
[53] F.O. Rice, K.F. Herzfeld, J. Am. Chem. Soc. 56 (1934) 284.
[54] P. Atkins, J. de Paula, Atkin's Physical Chemistry, 7th ed., Oxford University Press, 2002.
[55] B.E. Daikh, R.G. Finke, J. Chem. Soc., Chem. Commun. (1991) 784.
[56] B.E. Daikh, R.G. Finke, J. Am. Chem. Soc. 113 (1991) 4160.
[57] B.E. Daikh, R.G. Finke, J. Am. Chem. Soc. 114 (1992) 2938.
[58] B.E. Daikh, J.E. Hutchison, N.E. Gray, B.L. Smith, T.J.R. Weakley, R.G. Finke, J. Am. Chem. Soc. 112 (1990) 7830.
[59] B.E. Daikh, T.J.R. Weakley, R.G. Finke, Inorg. Chem. 31 (1992) 137.
[60] A.T. Blomquist, B.F. Hiscock, D.N. Harpp, J. Org. Chem. 31 (1966) 338.
[61] H. Irving, O. Weber, J. Chem. Soc. (1959) 2296.
[62] L.E. Manzer, Inorg. Synth. 21 (1982) 135.
[63] J.J. Felten, W.P. Anderson, J. Organomet. Chem. 36 (1972) 87.
[64] SHELXTL PC version 5.1, Bruker AXS, Madison, WI, 1997; G. Sheldrick, SHELX-97, Institut Anorg. Chemie, Tammannstr. 4, D37077 Göttingen, Germany, 1998.